Vrije Universiteit Brussel

FACULTEIT INGENIEURSWETENSCHAPPEN

Mechatronic Design of a Soccer Robot for the Small-Size League of RoboCup

Joris De Witte

Promotor: Prof. Dr. Ir. Bram Vanderborght

Eindwerk ingediend voor het behalen van de graad van Master in de Ingenieurswetenschappen: Werktuigbouwkunde

Academiejaar 2009-2010

Acknowledgments

At the end of my first year at the VUB, the course ‘mechatronica’ aroused my interest in robotic systems. During this course, a small robot was built to develop our skills in this matter. With the gained knowledge, I decided to choose the thesis subject of building a robot for the RoboCup Small Size League. I consider it as a privilege to be able to give a contribution in the development of these robots.

I would like to thank my promoter Dr. Ir. Bram Vanderborght for his support, guidance and enthusiasm for this subject. Many thanks go out to Jean-Paul Schepens and Ir. Ronald Van Ham for their time and help they gave along the way. Also, I would like to thank the people of the workshop: Marnix and Stijn for their technical assistance and sharing their experience.

As last, I would like to thank my family for their moral support.

The auteur:

Joris De Witte

Executive summaries

1. Mechatronisch ontwerp van een voetbalrobot voor de RoboCup Small Size League

In deze thesis wordt het mechatronisch ontwerp van een voetbalrobot behandeld. De robots die deelnemen aan deze competitie doorgingen in de loop der jaren een sterke miniaturisering. Het implementeren van alle componenten in een beperkte ruimte is dan ook de uitdaging van deze thesis.

Om een idee te hebben van de bestaande technologie werd voor iedere mechanische component een vergelijking gemaakt tussen de bestaande robots. Hieruit blijkt dat de deelnemende teams vergelijkbare componenten en technologieën gebruiken in hun robots. Toch kunnen enkele teams het verschil maken door een goed ontwerp en integratie van de componenten.

De ontworpen robot maakt gebruik van vier gelijkstroommotoren met elektronische commutatie voor de aandrijving. Via een tandwieloverbrenging wordt de kracht overgebracht naar de onmindirectionele wielen.

Om de bal weg te kunnen trappen, wordt een schietsysteem ingebouwd. Deze bestaat uit een veer die opgespannen wordt. Een sluitsysteem houdt de plunjer vast terwijl de veer wordt opgespannen. Een servomotor bedient dit sluitsysteem en kan de plunjer vrijmaken wanneer er getrapt moet worden.

Een dribbelsysteem brengt de bal naar het midden van de robot en houdt de bal ook voor de robot terwijl er gemanoeuvreerd kan worden met de robot. Deze bestaat uit een sneldraaiende cilinder dewelke een backspin geeft aan de bal.

Alle mechanische en elektronische systemen werden ontwikkeld en getest. Dit vormt een eerste stap naar het ontwikkelen van een complete robot, geschikt voor de deelname aan de RoboCup Small Size League hetgeen ook het doel is van deze thesis.

2. Mechatronic design of a soccer playing robot for the RoboCup Small Size League

In this thesis, the design of a soccer-playing robot is discussed. The robots that participate in this competition are a result of a strong miniaturization during the years. The implementation of all components in a limited amount of space is therefore the challenge of this thesis.

To have a notion of the existing technologies, a comparison was made between all competing robots for each mechanical component. This shows that the participating teams use similar components and technologies. Nevertheless, some teams can make the difference with well designed components.

The developed robot uses four brushless DC motors with electronic commutation for the drive unit. Via a spur-gear transmission, the power is transmitted to the omni-directional wheels.

To kick the ball, a shooting device is built. This system consists of a spring which is wound up. A lock/release system hold the plunger in place while winding up the spring. A servomotor actuates the lock/release system when a kick is required.

A dribbler device brings the ball to the center of the robot and hold the ball in front of the robot when it is maneuvering. The dribbler is a cylinder which spins with great speed and gives a backspin to the ball.

All mechanical and electronic components where developed and tested. This is a first step to developing a complete robot, fit for the RoboCup Small Size League which is the goal of this thesis.

Contents

List of figures

List of tables

1 Introduction

1.1 RoboCup

RoboCup[29] is a competition domain designed to advance robotics and artificial intelligence research through a friendly competition. Small Size robot soccer is one of the RoboCup league divisions. Small Size robot soccer, or F180 as it is otherwise known, focuses on the problem of intelligent multi-agent cooperation and control in a highly dynamic environment with a hybrid centralized/distributed control system. A Small Size robot soccer game takes place between two teams of five robots each. Each robot must be made conform to the dimensions as specified in the F180 rules: The robot must fit within an 180mm diameter circle and must be no higher than 150mm unless they use on-board vision. The robots play soccer with an orange golf ball on a green carpeted field that is 6.05m long by 4.05m wide. Robots come in two flavors, those with local on-board vision sensors and those with global vision. Global vision robots, by far the most common variety, use an overhead camera and off-field PC to identify and track the robots as they move around the field. The overhead camera is attached to a camera bar located 4m above the playing surface. Local vision robots have their sensing on the robot itself. The vision information is either processed on-board the robot or is transmitted back to the off-field PC for processing. An off-field PC is used to communicate referee commands and, in the case of overhead vision, position information to the robots. Typically the off-field PC also performs most, if not all, of the processing required for coordination and control of the robots. Communications is wireless and typically uses dedicated commercial FM transmitter/receiver units.

Figure 1: RoboCup competition layout

Building a successful team requires clever design, implementation and integration of many hardware and software sub-components into a robustly functioning system. This makes small-size robot soccer a very interesting and challenging domain for research and education.

1.2 Objectives

The design of a complete robotic system to compete in the RoboCup Small Size League involves the integration of different areas of knowledge.
In order to do so, a team with members of several Belgian universities is established. Each member works on a subproject which is related to their area of knowledge.

The goal of a first subproject is to develop a software platform for the high level control. All the strategic actions are embedded in the software. The software determines all the necessary actions the robots must undertake to win the game.
A second subproject has the goal of processing the data from the overhead camera. The location of each robot, the robots ID and the ball location have to be determined.
The goal of this thesis is to develop the mechatronic design of the small-size robot This robot houses all the systems to handle the ball and to communicate with the off-field PC. Before developing the robot, all requirements and limitations have to be known. In Appendix 1: the rules provided by RoboCup are summarized. These rules set the design specifications.
A first major component of the robot is the drive system which includes the motors, the transmission system and a set of omni-directional wheels. These are discussed in 'chapter 2: Drive Unit'.
The second component of the robot is a system to kick the ball. A state of the art of existing systems is discussed in 'chapter 3: Kicking device'. The benefits and disadvantages of all these systems are summarized. With this knowledge in mind, a new concept is developed.
Another component is the dribbler. This system has the task of giving a backspin to the ball. With this system, the robot is able to hold the ball in front of it and thus handle the ball better. This system is discussed in 'chapter 4: Dribbler'.
For this thesis, the electronics on board of the robot are all united into 'chapter 5: electronics'. This chapter discusses all the motor-controllers and a component for navigational purpose.
In order to control the robot some software has to be developed. The commands from the off-field PC have to be translated to the different motors on the robot. In 'chapter 6: Software', this is discussed.
The last chapter provides the conclusions and future work.

2 Driving unit

2.1 State of the art

Before discussing and constructing a drive system, the existing systems are reviewed. The next table gives an overview of these systems, currently used in robots competing in the RoboCup Small Size League. Top teams from the last three years are printed in bold. More information about the type of wheels can be found in next paragraphs.

Table 1: Comparison of RoboCup Teams: Driving unit

Team	Number of wheels	Type of wheels	Motors	Power	Speed	Spur gear ratio
Botania Dragon Knights [1]	4		Brushless DC	30 W		
Brocks [2]	4	Small	Brushless DC	30 W		3:1
B-Smart [3]	4	Small	Faulhaber 2342S006CR Brushed DC	20,5 W	9000 rpm	12:1
CMDragons [4]	**4**	**Small**	**Brushless DC**	**30 W**		
Eagle Knights [5]	4	Small	Faulhaber 2224P0212			14:1
ER-Force [6] (New system)	4	Small	Maxon EC 45 Brushless DC	30 W		
Field Rangers [7]	4	Small	Faulhaber 2232U009SR	9,35 W	7400 rpm	9,7:1
Immortals [8]	4	Small	Maxon EC 45 Brushless DC	50 W		45:12
Khainui [9]	4	Small	Namiki 22CL-3501PG80:1			10:1
KIKS [10]	4	Small	Maxon EC 45 Brushless DC			3,6:1

KN2C [11]	3	Small	Brushed DC		8160 rpm	13,6:1
ODENS [12]	**4**	**Small**	**Maxon RE-max 23 Brushed DC**	**11 W**	**8290 rpm**	**7,916:1**
OMID [13]	4	Small	Maxon EC 45 Brushless DC	30 W		5:1
Owaribito [14]	4	Small	Maxon RE-max 21 Brushed DC			
Parsian [15]	4	Small	Maxon EC 45 Brushless DC	30 W		4.7:1
RFC Cambridge [16]	4	Small	Brushless DC			
Robojackets [17]	3	Small	Maxon EC 45 Brushless DC			4,5:1
Robodragons [18]	**4**	**Small**	**Maxon EC 45 Brushless DC**	**30 W**		**3.047:1**
RoboFEI [19]	4	Small	Maxon EC 45 Brushless DC (Former Faulhaber 2232 DC)	50 W		3:1
RoboFighties [20]	2				2,16 m/s	
RoboPET [21]	4	Small	Maxon EC 45 Brushless DC	50 W		3,6:1
Skuba [22]	**4**	**Small**	**Maxon Brushless DC**	**30 W**		
MRL [23]	4	Small	Brushless DC			4:1
UBC Thunderbots [24]	4	Small	Maxon Brushless DC	30 W		3,5:1
Plasma-Z [25]	4	Small				

The most commonly used motor is a Maxon EC-45 brushless motor. These are very flat motors with a slightly larger diameter compared to brushed motors. They are very suitable for this application because of these specific dimensions. Most teams use a 30 Watt version, but some are already experimenting with more powerful versions like the 50 Watt versions. These teams are hoping for their robot to be faster and have more acceleration ability than their competitors.
Almost every team is using four wheels. This approach provides more space along the roll-axis of the robot. All teams who built their own omni-directional wheels are using the small wheels concept. This will be discussed in next paragraph.

2.2 Omni-directional wheels

2.2.1 Number of wheels

The number of wheels used on the robot depends on the available space and the desired amount of grip on the surface. Because the available space is limited, the number of wheels is limited to four. To have any stability, a minimum of three wheels is needed. Therefore, a choice between these two setups has to be made.

Table 2: Comparison between number of wheels

Four wheels	
Advantages	Disadvantages
- More space available along the roll axis of the robot - More grip can be achieved - One motor extra can provide additional power	- More expensive - More difficult to implement and control - Less space available in general - Contact between fourth wheel and ground surface uncertain
Three wheels	
Advantages	Disadvantages
- Less complex to implement and control -Less expensive - Always contact with ground surface	-Less grip -Less power

Almost all teams that are competing in the RoboCup Small Size league are using four wheels. The use of a kicking device makes a robot with three wheels difficult to built. More space is needed along the roll axis of the robot to implement the kicking device.

From this, it can be concluded that the use of four wheels is the best option in this application.

2.2.2 Dimensions of the wheel

The diameter of the wheel is directly related to the loss in ground surface. A simple calculation gives an idea of the influence of the wheel diameter.

The total ground surface is given by:

$$S_{total} = \pi . r^2 \tag{2.1}$$

With r the diameter of the ground circle of the robot.

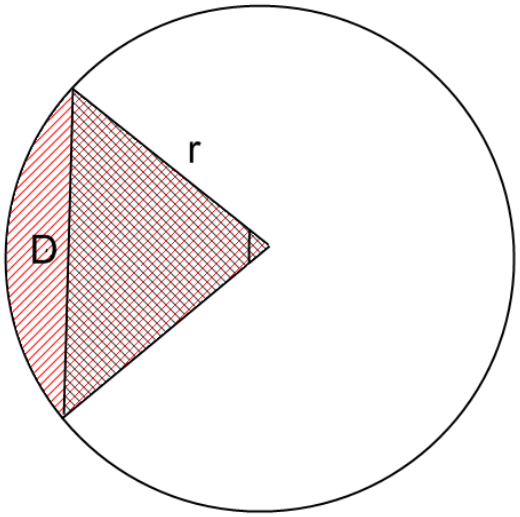

Figure 2: Calculation of loss in ground surface

The area of the partial circle shown in figure 2 is given by:

$$S_{partial\ \ circle} = \frac{r^2.\theta}{2} \tag{2.2}$$

With θ given by:

$$\theta = 2.\sin^{-1}(\frac{D}{2.r}) \tag{2.3}$$

The area of the triangle shown in figure 2 is given by:

$$S_{rectangle} = \frac{D}{2}.\sqrt{r^2 - \frac{D^2}{4}} \tag{2.4}$$

The loss in surface caused by the four wheels is given by:

$$4.\left(S_{partial\ \ circle} - S_{rectangle}\right) \tag{2.5}$$

In terms of percentage, the loss in surface becomes:

$$4.\frac{\frac{r^2.\theta}{2} - \frac{D}{2}.\sqrt{r^2 - \frac{D^2}{4}}}{\pi.r^2}.100\% \tag{2.6}$$

The loss of ground surface caused by an increasing diameter of the wheel is given in figure 3.

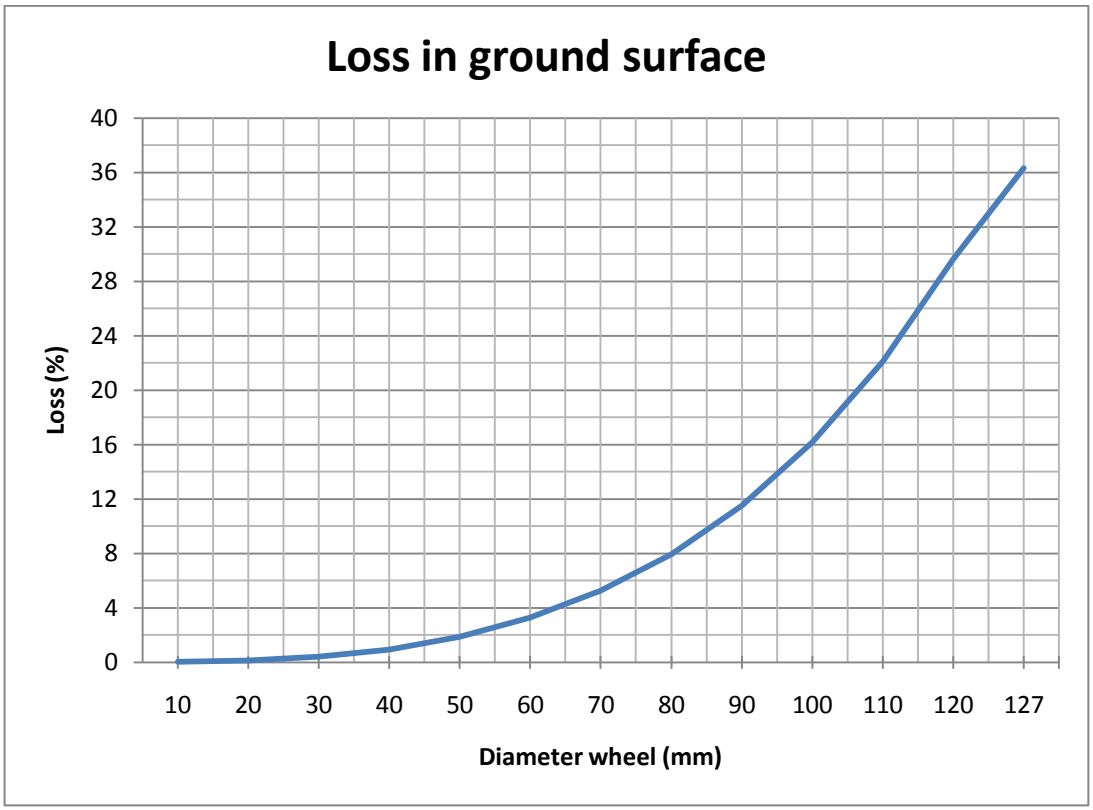

Figure 3: Loss in ground surface of the robot compared to wheel diameter

The loss of space caused by a wheel with diameter between 50 and 70 mm varies from 1,86% to 5,23%. A loss of 6% is equal to a rectangle with dimensions 45x33mm on the ground surface or is approximately the coverage of a Maxon EC 45 motor (see later). This loss is assumed acceptable. Because the calculation does not include the thickness of the wheels, a slightly smaller diameter should be selected. From this, it can be concluded that a diameter of 60 mm is a good option in this application.

2.2.3 Concepts of construction

There are many options to achieve an omnidirectional drive for the robot. In this paragraph, these options are summarized.

2.2.3.1 Purchase a ready to use wheel

These wheels are already tested. A good working of these wheels is guaranteed. The friction of the tangential wheels is limited.
There are also some disadvantages. The wheels are not custom made for this application. Also it isn't an innovative implementation for this application.

Figure 4: Rotacaster omniwheel

2.2.3.2 Small wheels design

This design is commonly used in most robots for the RoboCup Small Size league. It is a proven concept and can be custom made for the robot.
Again, it is not an innovative design anymore. The surface on the contour covered by the wheels is 25% which is relatively low.

Figure 5: Omniwheel-design by Parsian team[15]

Some experiments were executed by KIKS-team [10]. They experimented with different widths of tangential wheels.

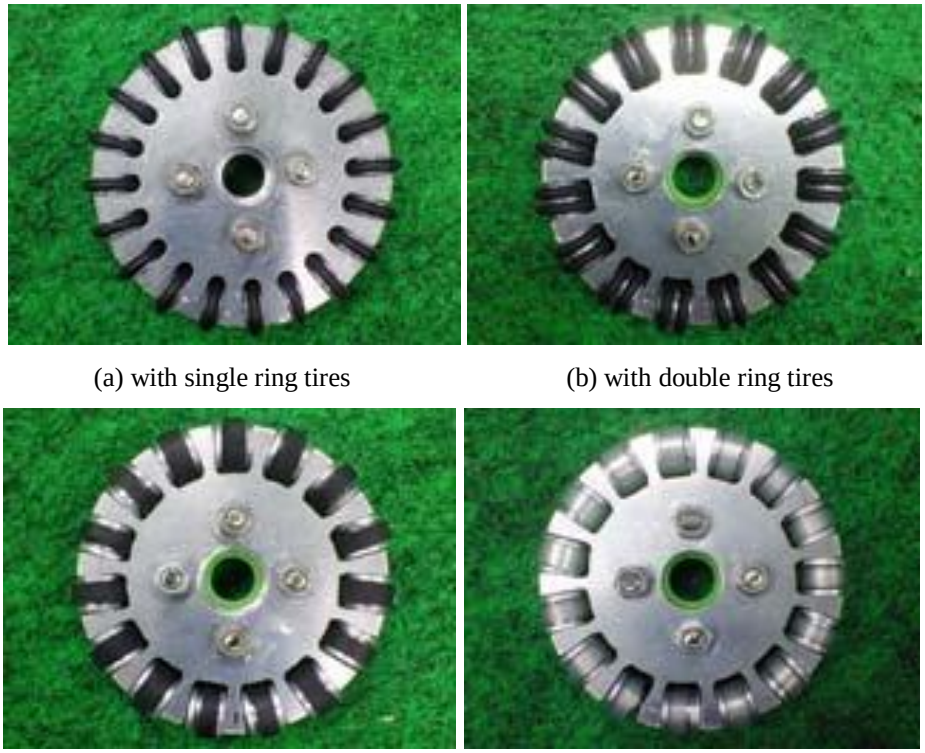

(a) with single ring tires (b) with double ring tires

(c) with thick rubber ring tires (d) with thick silicone rubber ring tires

Figure 6: Kiks research[10]: Various types of small wheels design

Various design types can be used. Design (a) has a low wheel to contour surface ratio. This means that the robot will bounce a lot when driving. Using design type (d), the bouncing of the robot can be reduced because the wheel to contour surface ratio is much higher in this case.

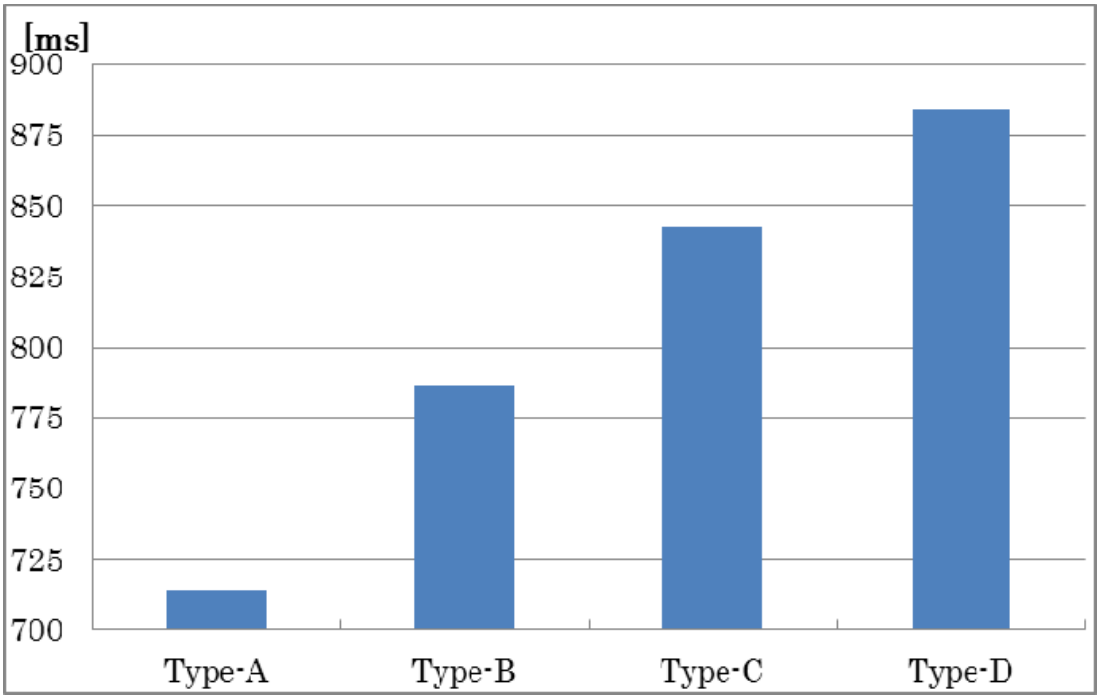

Figure 7:Kiks research[10]: Average time to reach 1m/s from static condition for the robot

Figure 7 shows the average time to reach 1m/s from static condition for the different wheels. It is clear that wheel design (a) is the best option when choosing for this type of design. The KIKS team has no explanation why type (a) is better than other designs while accelerating. A better acceleration means that type (a) has better grip (more efficient power transmission) and/or lower weight because F=a.m. This remark should be tested when a design is made for this application.

2.2.3.3 Concept by the Korea University

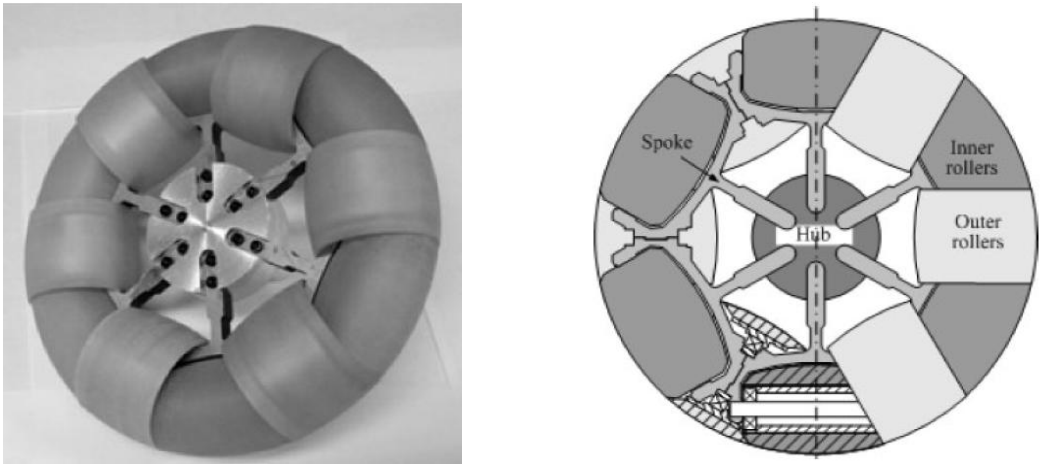

Figure 8: Omniwheel-design by Korea University [27]

This concept has been developed by the Korea University [27]. It has a wheel surface to contour ratio of 100%.

The resistance to contamination is poor. Because the robot will drive on a carpet surface, the danger exists that tiny particles will get stuck in the space between the tangential wheels.

It is very hard to construct these wheels especially when the diameter decreases. For this reason, this concept isn't suited for this application.

2.2.4 Final design

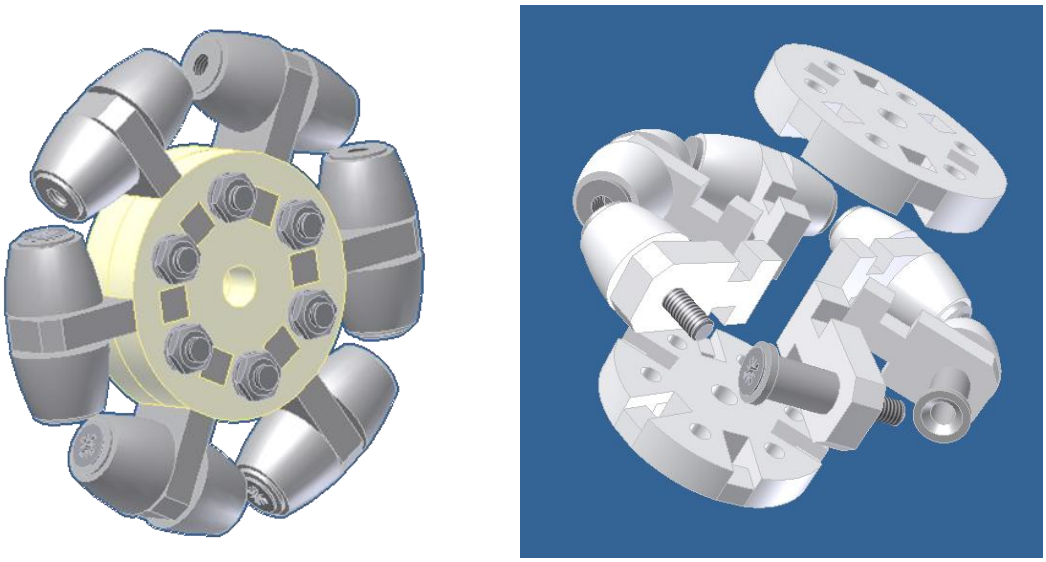

Figure 9: New omniwheel-design

This concept is a combination of concept 2 and 3. It uses slightly larger tangential wheels with a profile according to the contour of the wheel. The wheel surface to contour ratio can be increased to 52%.

This concept hasn't been proven yet but can be constructed with a small diameter. The omniwheels exist of two disks with grooves. In these grooves, pieces are placed to hold the tangential wheel axles. The wheels are than mounted on a bush. One bush has a hole through it and the other is threaded inside. These bushes are than bolted together with a small bolt.

The center disk has to be designed in two pieces. Otherwise, the whole structure can't be mounted together.

2.3 Driving Motors

The choice of the motors depends on the available space and required propulsion force. In the RoboCup Small Size League, large accelerations are needed to keep up with the other competing robots. It seems best to choose motors, similar to the motors of other teams to achieve a comparable acceleration. Most teams are using a brushless type of motor because these don't take a lot of space according to their power. A motor with following parameters was chosen.

- Maxon EC45 flat brushless motor
- Diameter: 45 mm
- Power: 30 Watt
- Supply voltage: 12V
- Starting current: 10A
- Nominal current: 2.8 A
- Stall torque: 255 mNm
- Nominal torque: 59 mNm
- Weight: 88 gr

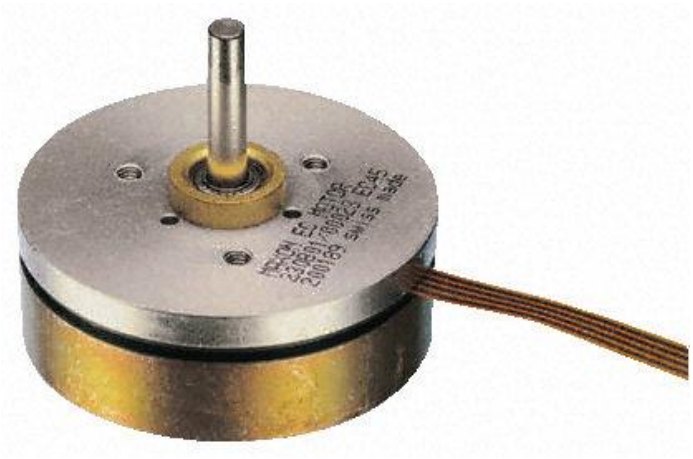

Figure 10: Maxon EC 45, 30Watt motor

2.4 Transmission unit

2.4.1 General

The power from the motors has to be transferred to the wheels. This can be achieved by directly connecting the motor to the wheels. In this case, the wheels have a diameter of 60mm and the motor a diameter of 45mm. With a direct connection, this leaves 7mm of ground clearance, which isn't much. Also, the space in the center of the robot isn't used optimal with a direct connection. By using a transmission system, more space at the front of the robot can be made available for other components by placing the motors towards the back of the robot.
A second, and more important, reason for the use of a transmission system is the reduction of motor speed. The motor has a no load speed of 4700 rpm which is very high for this application. The wheels have a diameter of 60mm thus the maximum speed of the robot would be 15 m/s or 54 km/h with a direct connection. A transmission system reduces the maximum speed while increasing the maximum torque on the wheels. This will have a positive influence on the acceleration of the robot. A transmission system is therefore a choice between maximum velocity and maximum acceleration.
The gear ratio used by competing RoboCup teams vary from 3:1 to 5:1. Most of them have slightly smaller wheels. Therefore, the gear ratio in this application should be at the higher side of the interval to have a similar velocity and acceleration.
There is not much information about the optimal gear ratio. Some teams [8] are now transferring to a 50W and lower gear ratio to have more velocity with the same acceleration. It seems best to consider this remark and choose a higher velocity than other competing teams.
In the next paragraphs, different types of transmission systems are discussed.

2.4.2 Spur gear

In table1 it can be seen that all teams use a transmission system with spur gears. This seems like the most obvious choice as a transmission system. These spur gears don't skid, which makes the control of the robot less difficult. When skid occurs, the control algorithm can't forecast the location of the robot anymore, because the encoders are mounted on the motors instead of on the wheels. Therefore, this transmission system is more reliable than other systems. For high gear ratio's, an internal spur gear can be used to reduce the required amount of space.

2.4.3 Belt transmission

Another system of transmission is a belt and pulley system. These are less reliable because they can skid. As said in previous paragraph, this makes a good control of the robot difficult. The flexibility of this system is an advantage. The pulley's can be produced using rapid prototyping. The belts can be made from a slightly elastic material which is available on a roll. The two ends of the belt can then be melted together. Therefore, each desired gear ratio can easily be achieved.

2.4.4 Final design

Before starting the design of the transmission system, some comments have to be made. The batteries used in the robot should be built in as low as possible to lower the center of gravity. Because the transmission units are at an angle relative to each other, a small space is created between these units. This space can be used to mount batteries to optimize the use of space. Figure 11 shows the integration of the batteries in the transmission unit. The batteries have a blue color in this figure.

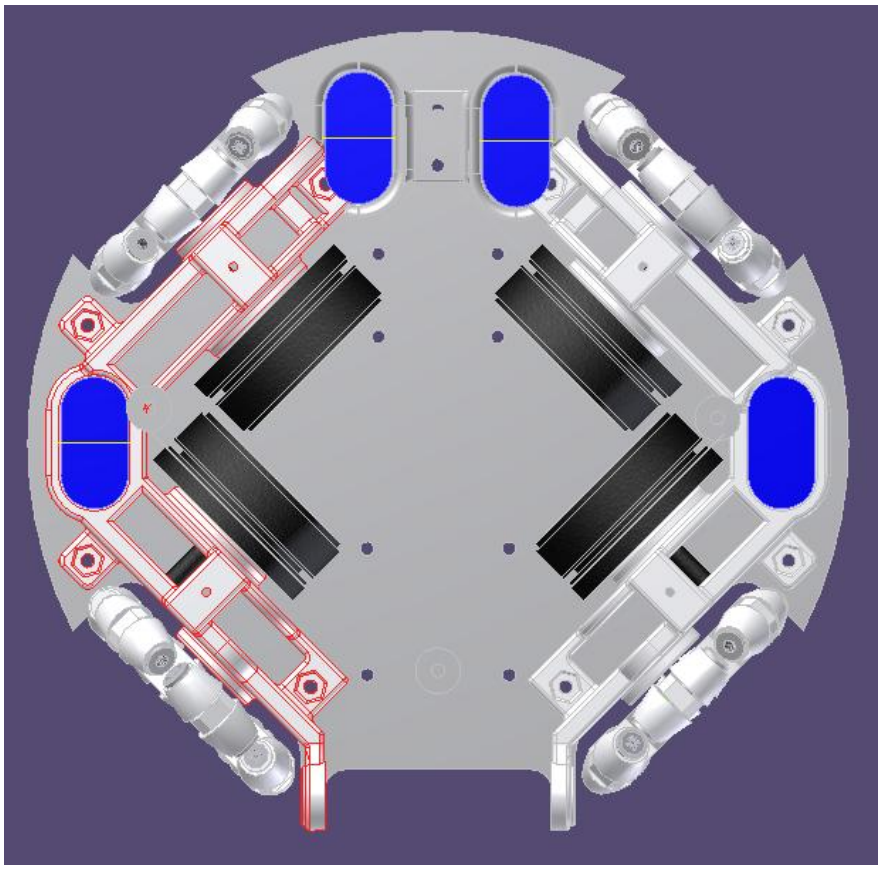

Figure 11: Structural design of transmission units

The four transmission units can be designed separately. This has a negative influence on the rigidness of the robot because they are not connected. To increase rigidness, the units on each side of the robot should be connected. Two separate structures which hold two motors, wheels and transmission system are therefore created. By opting for two separate structures, more space is available for the kicking device and dribbler than in case of one large structure. Figure 12 and 13 show a close-up of the transmission structure, one with a spur gear and the other with a pulley.

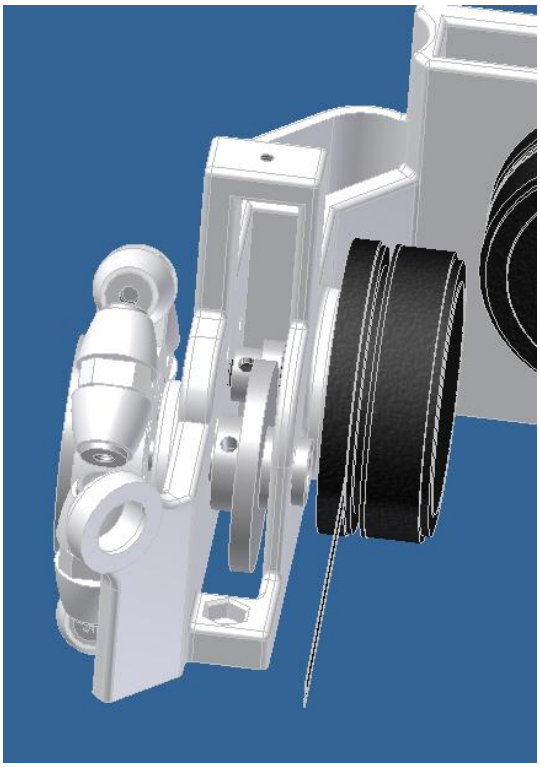

Figure 12: Close-up of front transmission unit with spur gears

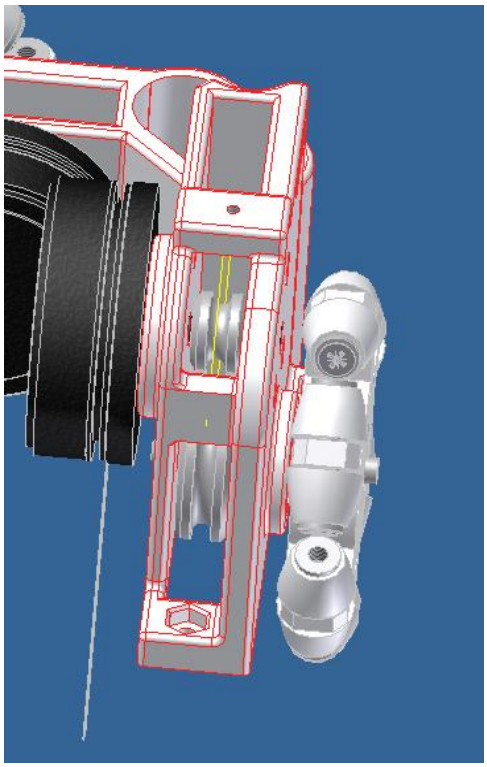

Figure 13: Close-up of rear transmission unit with pulley

2.5 Experiments

During the first tests, it was seen that not all of the contact points of the wheels with the ground surface were located in one plane. This causes at least one wheel to lose some grip. This can cause problems for the control software.
A solution for this problem is to suspend the wheels like in other vehicles. The suspension system could also reduce the bouncing of the robot due to the non-circular wheels.
An experiment was performed to test the belt and spur gear transmission. The belt transmission skids while driving. This isn't the case with the spur gear transmission. Therefore, it is concluded that the spur gear transmission is the best option for this application.

2.6 Conclusions

In this chapter, the drive unit was discussed. From a comparison between all competing teams, it can be concluded that almost all teams use four wheels. This provides extra space along the roll axis of the robot to implement a shooting system. Therefore, four wheels are used in this application.
There are several possible designs for the omni-directional wheels. The competing teams all use a similar wheel design with small tangential wheels. For this application, a new concept was developed with larger tangential wheel. Therefore, a higher wheels surface to contour ratio is obtained.
The motors used by the competing teams have a power rating varying from 30 to 50 Watts. In this application a 30 Watt EC45 Maxon motor is used, which is a commonly used motor in the RoboCup Small Size competition. This motor powers the wheels via a transmission unit. In this application, two principles of transmission are reviewed. From tests, it is concluded that a spur gear transmission is the best option. This transmission doesn't skid like the belt transmission.

3 Kicking device

3.1 General

There are several designs used by competing RoboCup Teams. The design parameters for a shooting device are the following:

- Efficiency
- Cost
- Weight
- Required space
- Time between shots
- Number of shots
- Safety
- Variable force

3.2 State of the art

Table 3: Comparison between RoboCup teams: Kicking device

Team	Device type	Ball speed	Chip-kick device (distance in the air)
Botania Dragon Knights [1]			
Brocks [2]	Solenoid		
B-Smart [3]			
CMDragons [4]	**Solenoid**	**15 m/s**	**4,5 m**
Eagle Knights [5]	Solenoid		
ER-Force [6] (New system)	Solenoid	8 m/s	
Field Rangers [7]	Solenoid	10 m/s	6 m
Immortals [8]	Solenoid		
Khainui [9]	Solenoid		
KIKS [10]	Solenoid		

KN2C [11]	Solenoid		
ODENS [12]	Solenoid		
OMID [13]	Solenoid	8 m/s	
Owaribito [14]	Solenoid	10 m/s	
Parsian [15]	Solenoid		5 m
RFC Cambridge [16]	Solenoid		
Robojackets [17]	Solenoid		
Robodragons [18]	Solenoid		
RoboFEI [19]	Solenoid		
RoboFighties [20]			
RoboPET [21]	Solenoid	10 m/s	
Skuba [22]	**Solenoid**	**14 m/s**	7,5 m
MRL [23]	Solenoid		
UBC Thunderbots [24]	Solenoid	8 m/s	
Plasma-Z [25]	Solenoid		

From table 3 it can be concluded that all teams which use a shooting system have opted for a solenoid system. In the past, the Philips CFT team [28] used a mechanical spring actuated system. Back then, larger dimensions of the robot were allowed. Such a system was easier to implement because of these dimensions.

3.3 Types of shooting devices

The electrical energy stored in the batteries has to be transformed in mechanical energy to move the ball. This can be accomplished in different ways.

3.3.1 Solenoid actuated

In this system, self-inductance is used. A current is send through a coil which generates a magnetic field. This field can be increased by increasing the number of windings of the coil or by increasing the current through the coil. With this magnetic field, a ferromagnetic material can be attracted or repulsed.

Most solenoids available in stores are not suitable for this application. They work on low voltage and are very slow. The force they develop is rather low. This results in low ball velocities. In order to kick the ball at high velocities, a high voltage solenoid is required. These aren't available in stores yet so they have to be built a custom to the application. With these high voltage solenoids, ball speeds of up to 10 m/s are no exception.
The dimensions of the system depend on the design. For this application, typical values are the following [14]:

- A total mass of up to 200 gr
- Ball speeds of more than 10m/s
- 200 volt circuit
- 3700 µF capacitors

This system is very flexible in terms of creating a variable shooting force. The time to reload can be kept low. The number of shots is only limited by the state of the battery.
The most important disadvantages are the safety risks involved in using high voltage. Also, a lot of heat is generated when activating the system. This heat has to be evacuated out of the robot. Another disadvantage is the required space for the capacitors and the weight of the coil.
Most competing teams at present use this system. Many developments are made in terms of reducing the weight and increasing the power of the system. This system has been tested with success by many teams.

3.3.2 Spring actuated

This system is based on the storage of energy in a spring. It has two major functions. The first function has the task of winding the spring up. The second function is a lock/release system to hold the plunger in his place while winding up and releasing the spring when needed.

This system is more safe then the solenoid system because there is no high voltage present. With a well designed system, the cost and required space can also be reduced. When friction is reduced, very high efficiency can be achieved because there is a direct connection from the motor to the spring. The number of shots is only limited by the state of the batteries.
The major disadvantage is the reload time. It takes a powerful motor to reload the system in a short time. A variable shooting force can be achieved but again, it takes time to set the spring at this desired force.

3.3.3 Pneumatic actuated

In the past, a lot of the teams used a pneumatic actuated system [28]. The air pressure is retrieved from a large air tank on the robot that is pressurized before the match. Pneumatic cylinders are connected to a solenoid actuated valve which controls the airflow.
A big disadvantage of this system is the large air tank that has to be built in.
The number of shots depends on the volume of the tank and the pressure inside the tank.

3.3.4 Other

A lot of other systems can be designed for the purpose of shooting the ball. Most of these systems have several major flaws.
For instance a rack and spur device can be used. This system needs a large motor with huge power ratings.

3.4 Shooting system model

3.4.1 General

For this application, it was decided to construct a spring actuated shooting device. To wind the spring up, a spindle with nut is used. The nut presses against the spring which is thereby compressed. A lock and release mechanism holds the plunger in place and releases it when needed.
The modeling of the shooting system will be divided into three parts. A first part is determining the maximum force the motor can deliver. Based on this value, a spring can be selected in the second part. In this part, the time needed for the winding of the spring is modeled. The third part will determine the parameters needed to model the actual shooting process.

3.4.1.1 Force in spindle

The force that can be generated to compress the spring depends on the applied torque on the spindle. With following formulas, this can be calculated. [26]

$$T = F.\frac{d_2}{2}.\tan(\varphi \pm \rho') \qquad (4.1)$$

With:

- F longitudinal force in the axis
- d_2 pitch diameter of the screw thread
- ϕ lead-angle of the screw thread
- ρ' screw thread friction angle.
  - \+ for tightening
  - \- for releasing

Reforming formula 4.1 with the force on the right hand side:

$$F = \frac{T.2}{d_2.\tan(\varphi \pm \rho')} \qquad (4.2)$$

3.4.1.2 Compression process

Using the stall torque of the motor in formula 4.2, a spring can be selected to use in the application. The parameters of the spring are the following:

- $F_{spring} = Force\ in\ the\ spring\ when\ compressed$
- $l_f = Free\ length$
- $l_c = Compressed\ length$

With these parameters, the compression parameters can be calculated. These parameters are the force in the spring while compressing, the rotation speed of the motor and the compression time.
A force function can be found according to the compressed length (x) of the spring:

$$F_{spring} = k.x \tag{4.3}$$

From this force function, a rotation speed function can be derived. The relation between the motor torque and rotation speed according to the maxon datasheet [31] is given by:

$$n = n_0 - \frac{n_0}{M_H}.M \tag{4.4}$$

With:

- n_0: No load rotation speed
- M_H: Stall torque
- n: Rotation speed of the motor
- M: Torque of the motor

The rotation speed of the motor can be expressed as a function of the spring compression 'x' using formula 4.2, 4.3 and 4.4. Rotation speed is expressed in revolutions per second.

$$n = n_0 - \frac{x.k.d_2.n_0.\tan(\varphi \pm \rho')}{2.M_H} \tag{4.5}$$

With this rotation speed function, the time needed to wind the spring up to a compressed length of 'r' can be calculated. When the spring is compressed an infinite part dx with rotation speed n, the time needed to do this is given by:

$$dt = \frac{dx}{n.a} \tag{4.6}$$

The total time needed to compress the spring to length 'r' can be calculated.

$$t = \int_0^r \frac{dx}{n.a} \tag{4.7}$$

This results in:

$$t = \frac{-2.M_H}{k.d_2.\tan(\varphi \pm \rho').n_0.a}.\ln\left|1 - \frac{r.k.d_2.tan(\varphi \pm \rho')}{2.M_H}\right| \tag{4.8}$$

3.4.1.3 Releasing process

In this paragraph, the releasing process is discussed. It is assumed that the process will take place in three phases. In the first phase, the plunger will move towards the ball without touching it. The second phase is the moment of impact between the plunger and the ball. At this time, the preservation of impulse law can be used. For the third phase, it is assumed that the ball and plunger will move together. Therefore, the spring accelerates the combined system of plunger and ball. In the actual system, it is possible that the ball will move faster than the plunger. The velocity of the ball will be greater than the calculated one in this case. Therefore, the model gives a worst case scenario.

At the of the third phase, the shooting velocity of the ball is reached.

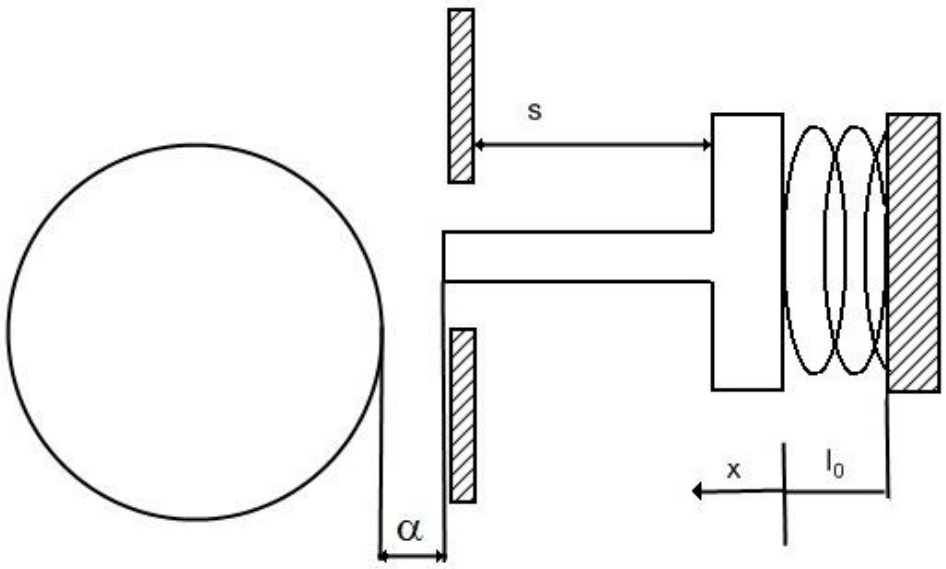

Figure 14: Shooting system release process parameters

The following parameters will be used to perform the calculation:

- $F_0 = Spring\ force\ before\ releasing$= k.$l_0$
- $s = total\ stroke\ length$
- $x = position\ of\ the\ plunger$
- $F = force\ in\ the\ spring\ at\ position\ x$
- $k = spring\ stiffness$
- $\alpha = plunger\ offset$

A. <u>Only plunger moves</u>

To make the results more logic, the origin of the x-axis is changed. It is now assumed that x is zero at the start of the releasing-process. The force in the spring is function of x:

$$F = k.(l_0 - x) = F_0 - k.x \tag{4.9}$$

The acceleration is given by:

$$a = \frac{F}{m_{plunger}} = \frac{F_0 - k.x}{m_{plunger}} \tag{4.10}$$

In order to solve this problem, a differential equation has to be solved:

$$m_{plunger}\ .\ddot{x} + k.x = F_0 \tag{4.11}$$

The solution of this equation has following form:

$$x(t) = Acos(\omega t) + Bsin(\omega t) + C \tag{4.12}$$

With:

$$\omega^2 = \frac{k}{m_{plunger}} \tag{4.13}$$

The boundary conditions are:

$$x(0) = 0$$
$$v(0) = 0$$
$$a(0) = \frac{F_0}{m_{plunger}}$$

Filling in these boundary conditions leads to values of A,B,C:

$$x(t) = \frac{F_0}{k}.(1 - \cos(\omega t)) \tag{4.14}$$

$$v(t) = \frac{F_0}{k}.\omega.\sin(\omega t) \tag{4.15}$$

$$a(t) = \frac{F_0}{m_{plunger}}.\cos(\omega t) \tag{4.16}$$

B. Impact

The value of x where impact occurs is noted as 'α'. From formula 4.20, the time t1 of impact can be determined:

$$\alpha = \frac{F_0}{k}.(1 - \cos(\omega t_1)) \tag{4.17}$$

$$\cos(\omega t_1) = 1 - \frac{k.\alpha}{F_0} \tag{4.18}$$

$$\omega.t_1 = \cos^{-1}(1 - \frac{k.\alpha}{F_0}) \tag{4.19}$$

With formula 4.23, the velocity right before impact becomes:

$$v_{t1} = \frac{F_0}{k}.\omega.\sin\left(\cos^{-1}(1 - \frac{k.\alpha}{F_0})\right) \tag{4.20}$$

$$v_{t1} = \frac{F_0}{k}.\omega.\sqrt{1 - \left(1 - \frac{k.\alpha}{F_0}\right)^2} \tag{4.21}$$

$$v_{t1} = \sqrt{\frac{2.\alpha.F_0 - k.\alpha^2}{m_{plunger}}} \tag{4.22}$$

At the moment of impact, the conservation of impulse law can be used to determine the velocity after the impact.

$$m_{plunger}\ v_{plunger\ ,t1} + m_{bal}\, v_{bal,t1} = (m_{plunger}\ + m_{ball}).\, v_{t2} \tag{4.23}$$

Assuming that the velocity of the ball is zero before impact:

$$v_{t2} = \frac{m_{plunger}\ v_{plunger\ ,t1}}{m_{plunger}\ + m_{ball}} \tag{4.24}$$

$$v_{t2} = \frac{m_{plunger}\ \sqrt{\frac{2.\alpha.F_0 - k.\alpha^2}{m_{plunger}}}}{m_{plunger}\ + m_{ball}} \tag{4.25}$$

C. <u>Accelerating plunger and ball</u>

This calculation is similar to those made in section A. The mass becomes the combined mass of plunger and ball. Only the start conditions of the differential equation change. Variable 'x' is equal to α at the start. The velocity is equal to v_{t2} at the start and the acceleration at the start becomes:

$$\frac{F_0 - k.\alpha}{m_{total}}$$

$$x(t) = \left(\alpha - \frac{F_0}{k}\right).\cos(\omega t) + \frac{v_{t2}}{\omega}.\sin(\omega t) + \frac{F_0}{k} \tag{4.26}$$

$$v(t) = \omega.\left(\frac{F_0}{k} - \alpha\right).\sin(\omega t) + v_{t2}.\cos(\omega t) \tag{4.27}$$

$$a(t) = \omega^2.\left(\frac{F_0}{k} - \alpha\right).\cos(\omega t) - v_{t2}.\omega.\sin(\omega t) \tag{4.28}$$

3.4.2 Application note

In this paragraph, the mathematical model is applied on the shooting system of the robot. For this application, following components will be used.

Table 4: Shooting system components

Motor:	Steel Spindle:	Plunger:	Spring:
P=2.5 watt	M3	mass=140gr	F=300N
$n_{0:}$11400	a=0.5mm		lf=50 mm
M_H: 8,52mNm	l=30mm		lc=30 mm
Gear ratio: 1/17	d2=2.675mm		
	ϕ=3. 41°		
	ρ'=12°		

The motor that is used was already available and will be used for testing purposes. When this motor is proven insufficient, another one can be mounted.
The diameter of the spindle is kept as low as possible because it acts as a sort of reduction for the motor. Using the spindle as a reduction results in a more compact design.

3.4.2.1 Spring selection

In order to select a spring, the maximum achievable force has to be determined:

$$F_{max} = \frac{M_H . 2}{d_2 . \tan(\varphi \pm \rho')} = 392\ N \qquad (4.29)$$

When this maximum force is used to select an imaginary spring, the time to wind the spring up can be calculated using formula 4.8. The spring stiffness 'k' is given by:

$$k = \frac{F_{max}}{l} = \frac{392\ N}{20\ mm} = 19644\frac{N}{m}$$

With l: the length of the spring which is determined by the shooting system design. The result is shown in figure 14.

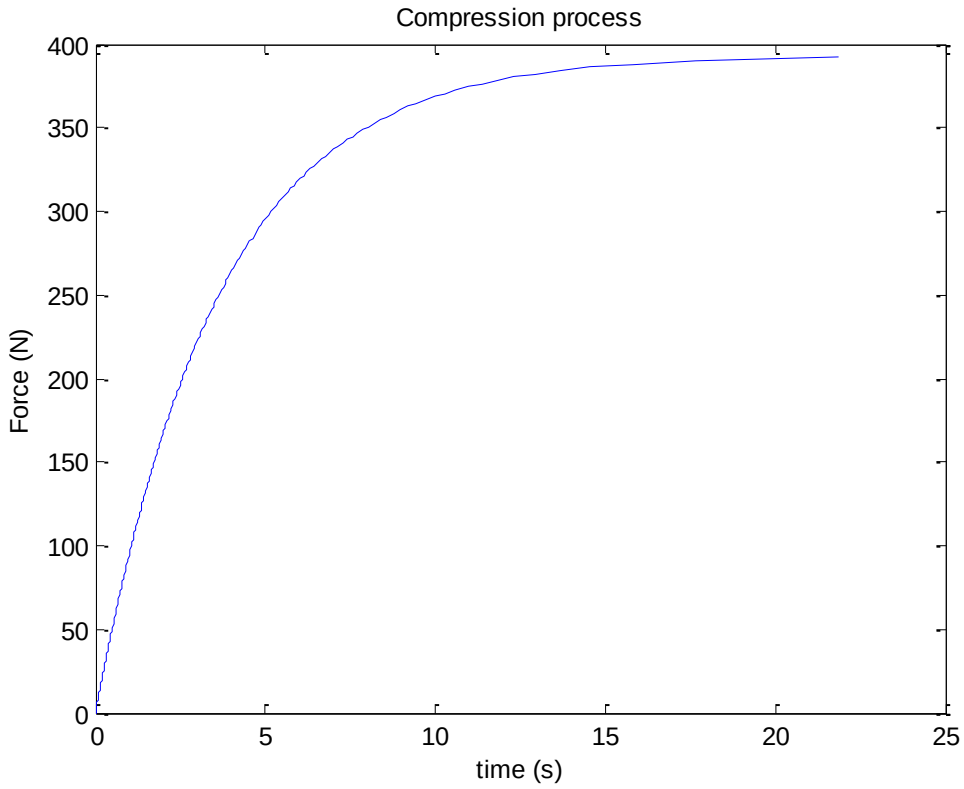

Figure 15: Compressed spring length as function of the time

When a spring is selected with a compressed force close to the maximum achievable force of the motor, the time to compress the spring will increase rapidly. It is seen in figure 15 that a force of 350 N is reached, the time to compress the spring further increases rapidly.

In this application note, a maximum force of 300 N is used to reduce the compression time. This is a difference of 24% relative to the maximum force. The parameters of the spring are the following:

- The stiffness becomes 17700 N/m.
- The difference between free length and compressed length is 20 mm.

3.4.2.2 Compression process

The time to wind this spring up can be determined using formula 4.8 :

$$t = \frac{-2.M_H}{k.d_2.\tan(\varphi \pm \rho').n_0.a}.\ln\left|1 - \frac{r.k.d_2.tan(\varphi \pm \rho')}{2.M_H}\right| = 6{,}8\ s$$

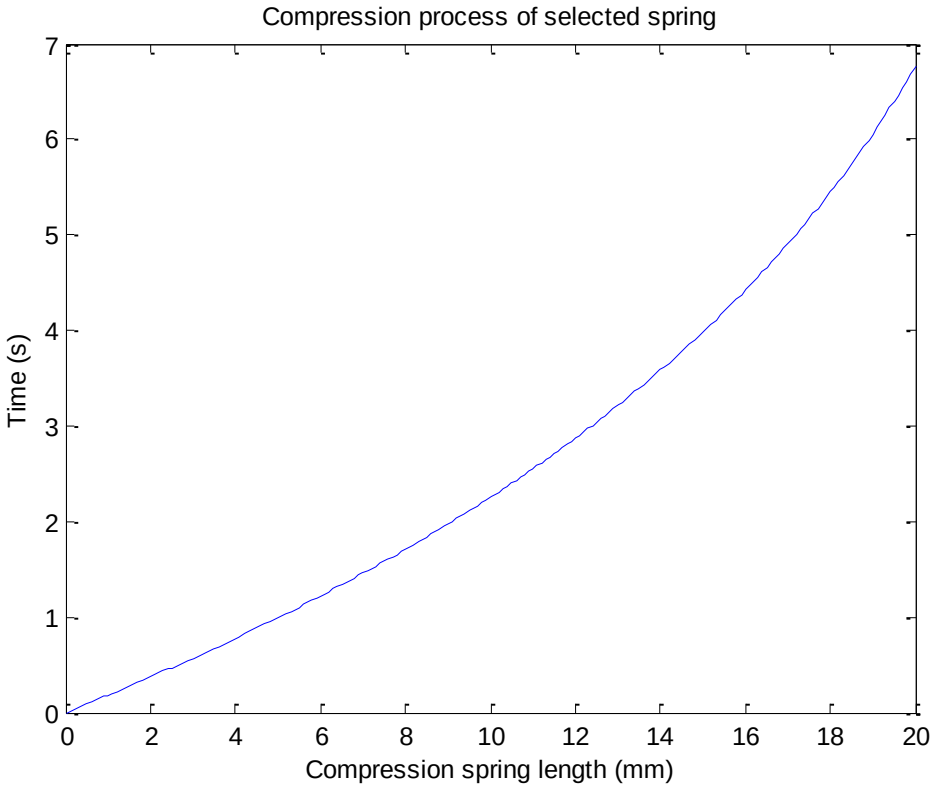

Figure 16: Compression time with selected spring

In figure 16, the time to compress the spring is given in function of the compressed length. The compressed length is proportional to the force. Therefore, the graphic which represents the time in function of the force is similar to figure 16.
The time needed to wind the spring up is relatively high. A reduction of this time can be achieved by pre-compressing the spring. In this case, it has to be considered that the force in the spring cannot start from zero. This implicates that the shooting system is not fully variable but has a minimum shooting velocity. In a later stage of

the project, a more powerful motor should allow to reduce this time. The selected components will be used for testing purposes and to verify the mathematical model.

3.4.2.3 Releasing process

In this paragraph, the releasing process is discussed. The force at the start of the release is set at the maximum compressed force of the spring.

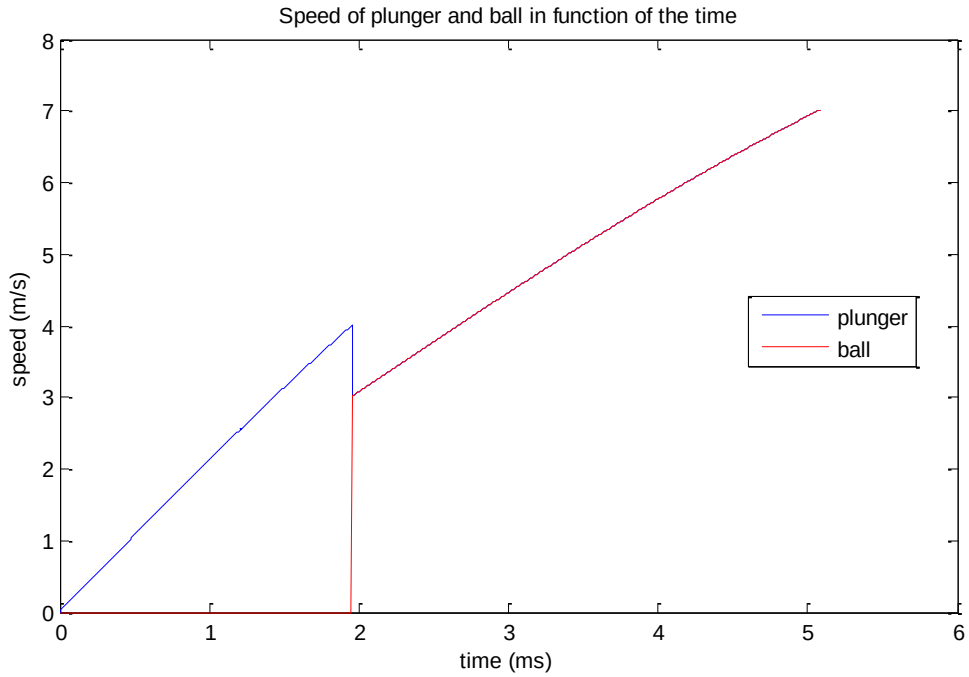

Figure 17: Plunger and ball speed as function of time

In figure 17, the plunger velocity is given as function of the time. At approximately 2 ms, the speed drops because of the impact with the ball. From that time, the plunger speed is equal to the ball speed. The final speed of the ball is equal to 7m/s. This is lower than the goal of 10 m/s. Again, this setup will be used for testing purposes. When a good design is created, a more powerful motor can be mounted.

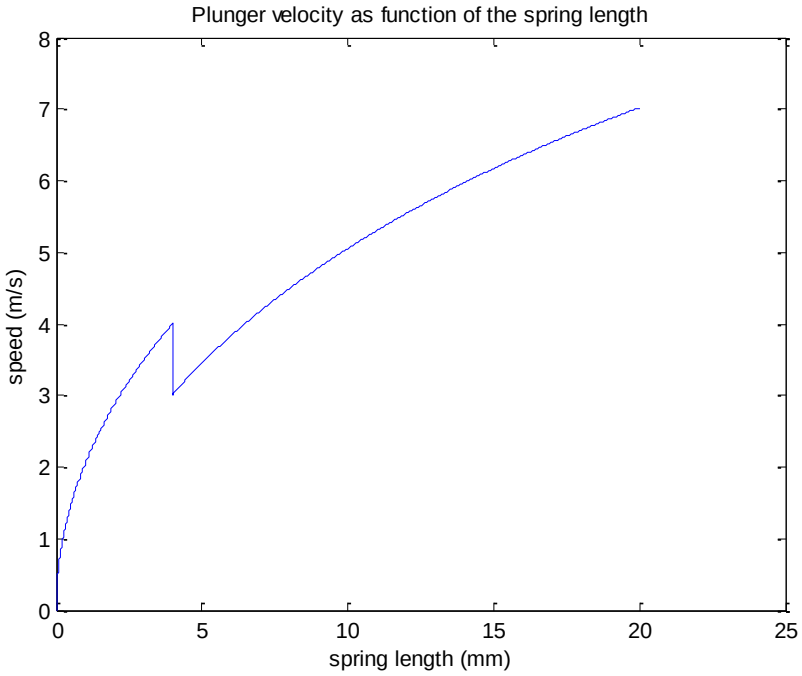

Figure 18: Plunger velocity as function of the spring length

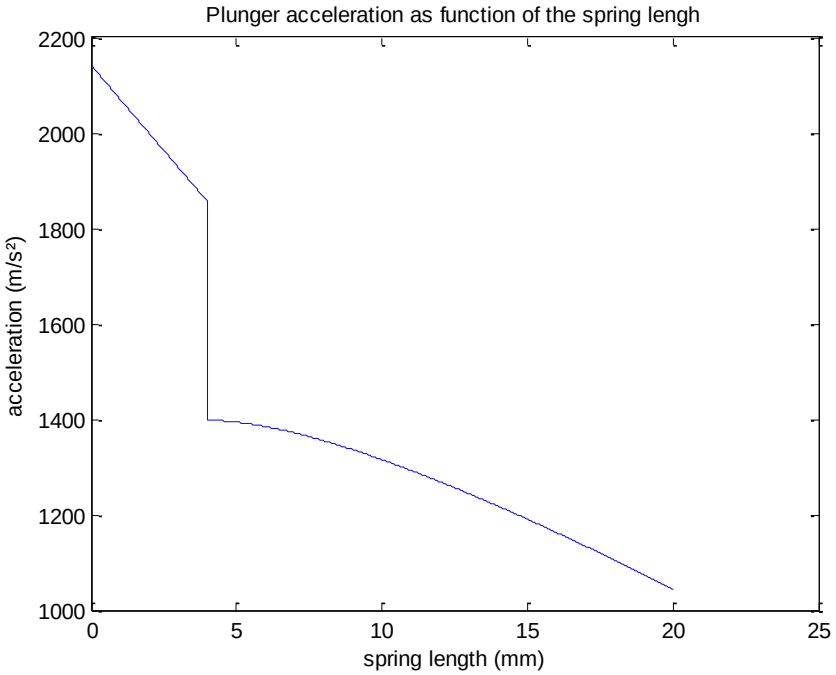

Figure 19: Plunger acceleration as function of the spring length

3.4.2.4 Optimizing plunger weight

By changing the plunger's weight, a higher ball velocity can be obtained. Figure 20 shows the effect of the plunger mass on the ball velocity. The maximum force of the spring was set at 300N.

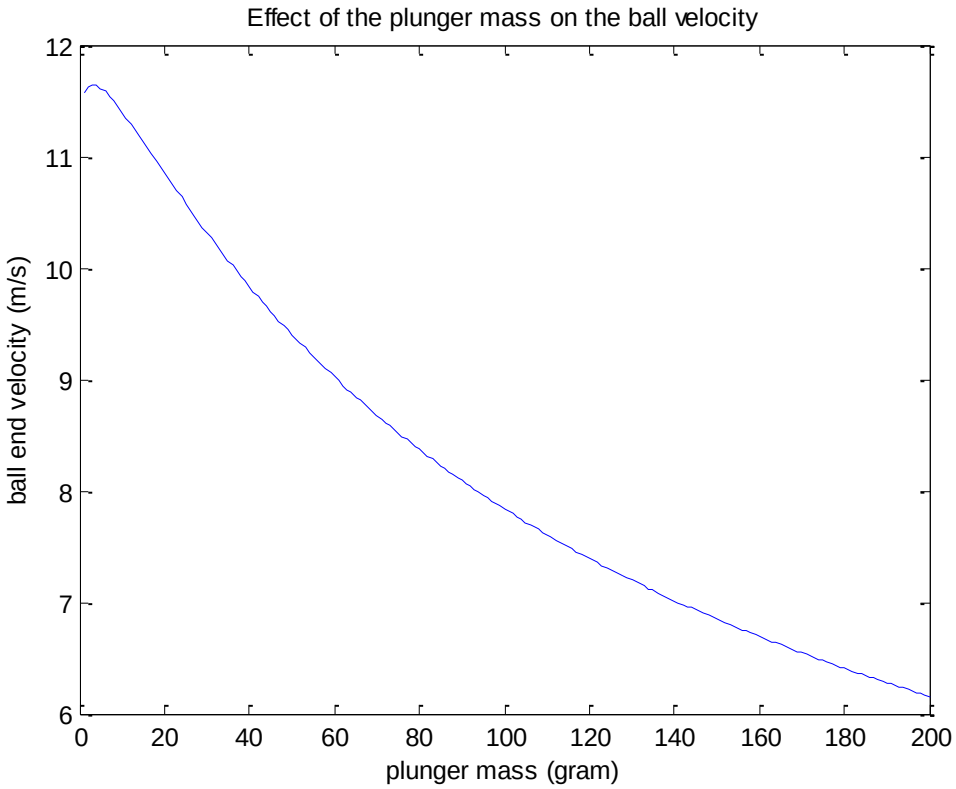

Figure 20: Ball velocity as function of plunger mass

From this graph, it can be concluded that the mass of the plunger should be kept as low as possible. A velocity of 10m/s can be achieved with a plunger mass lower as 40 gram.

3.4.2.5 *Effect of the plunger offset α*

In this paragraph, the effect of the plunger offset (α) relative to the ball is discussed. This offset is the distance between the ball and the plunger at the start of the releasing process.

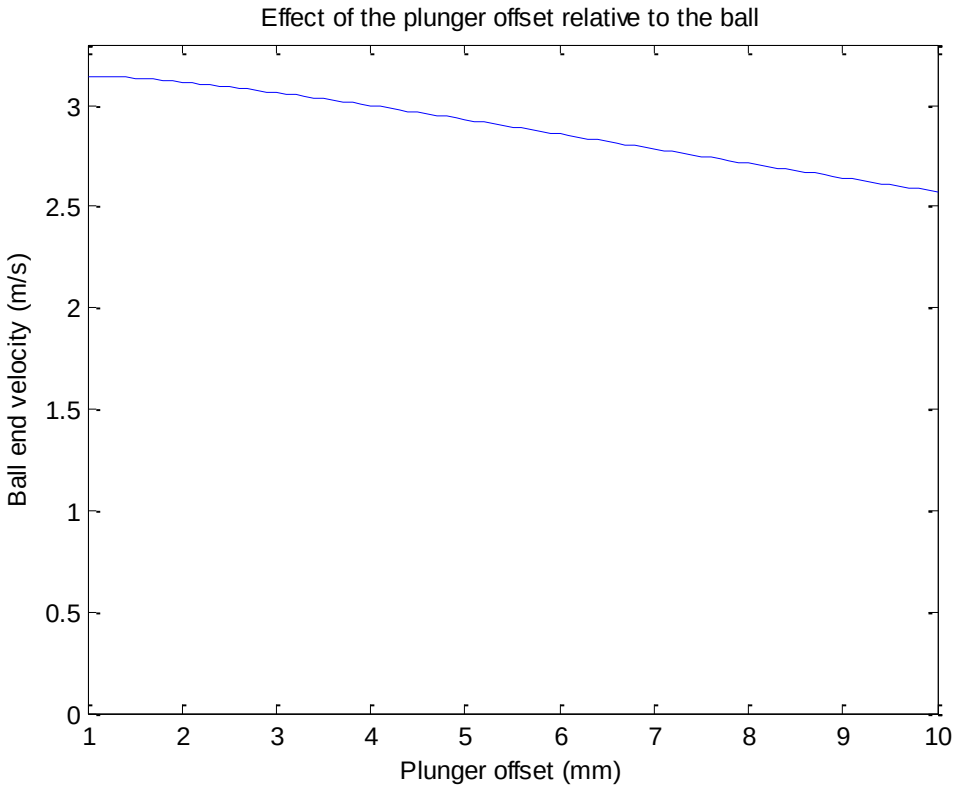

Figure 21: Effect of the plunger offset

Figure 21 shows that there is an effect of the plunger offset on the end velocity of the ball. It seems best to keep the offset as low as possible.

3.5 First construction

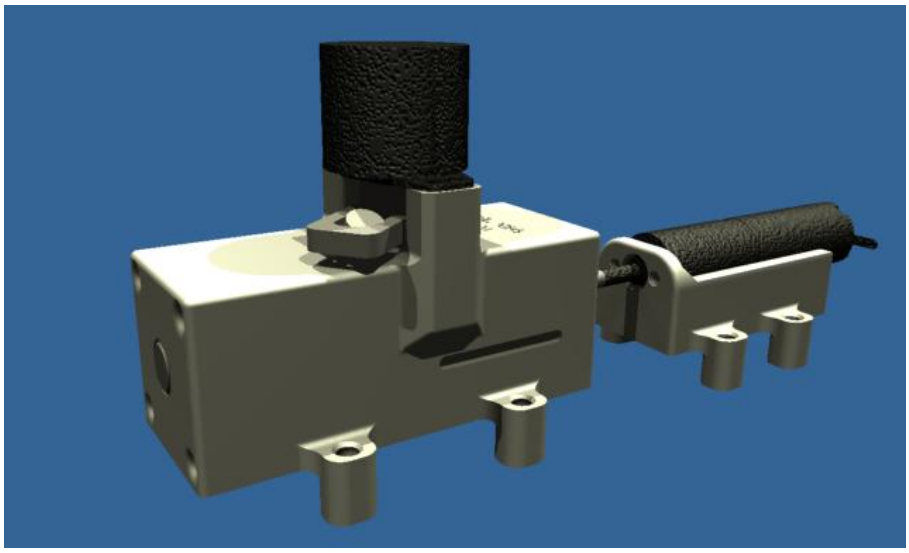

Figure 22: First shooting system, general overview

In this paragraph, a first design concept is discussed. The DC motor is mounted directly onto the spindle (see figure 23). In this case, the spindle has a diameter of 3mm in order to achieve a large reduction ratio between the motor speed and linear displacement of the spring. The spindle is threaded with a triangular M3 screw thread.

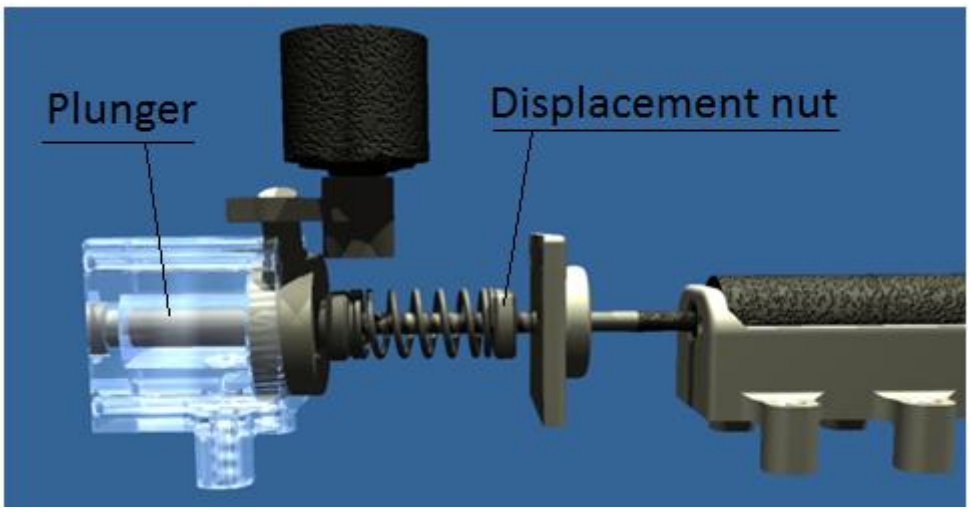

Figure 23: First shooting system: view on the spindle

A nut is mounted on the spindle to achieve the linear displacement (see figure 24). The nut has a specific profile which fits into a guidance bush. The profile makes sure that the nut cannot turn in the guidance bush. Otherwise, there would be no linear displacement.

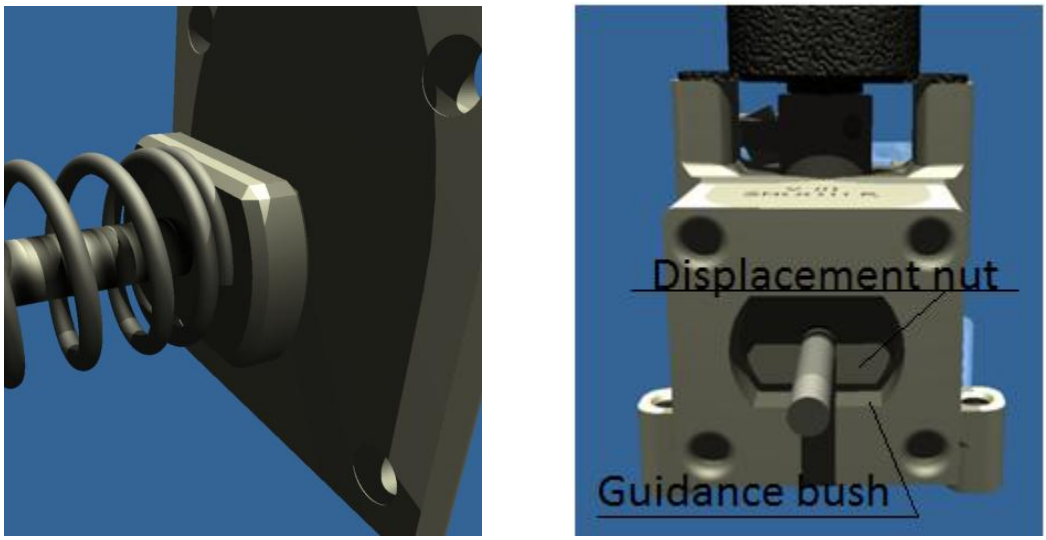

Figure 24: First shooting system: close-up on the displacement nut (left) and guidance bush (right)

The spring is mounted between the displacement nut and the plunger. To hold the spring in place, the spindle is made long enough so that the plunger will never lose contact with the spindle. Therefore, the spring can never get off the plunger.

To hold the plunger in place while winding the spring up, a lock/release mechanism is made (see figure 25). This is achieved by cutting the profile of the plunger out of a ring. When the ring is turned relatively to the plunger, the profile will also be turned. Therefore, the plunger can only get through the ring when the profile is exactly in the right position. A stepper motor will actuate this ring to release the plunger.

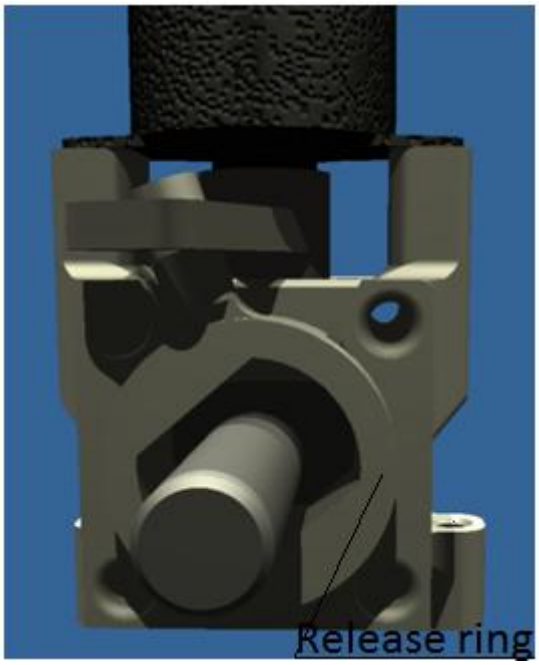

Figure 25: First shooting system, close-up on the release ring

3.6 Second construction

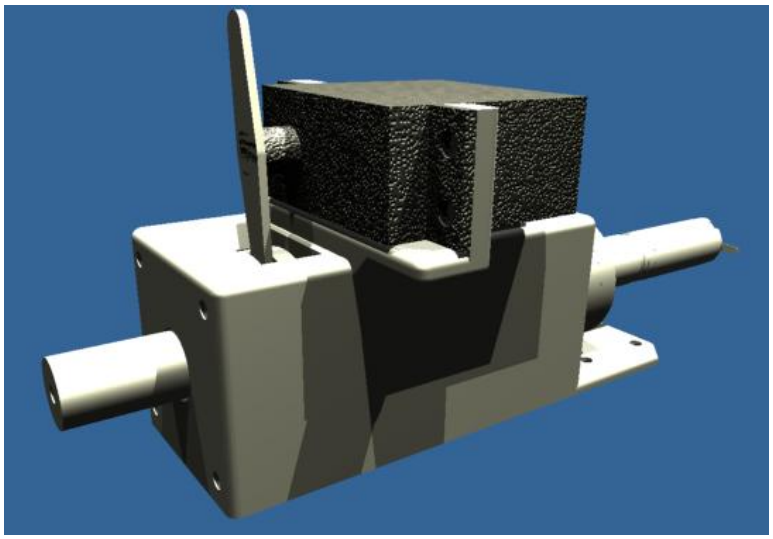

Figure 26: Second shooting system, general overview

In this first design, a lightweight plunger is used. Because the mathematical model wasn't finished when the design was made, a second construction was built with a

heavier plunger to test the effects. The working principle is the same, only the dimensions were enlarged. The large plunger is more difficult to place in the limited amount of space. Therefore, the winding mechanism is fit into the plunger to save space. This is seen in figure 27, where the lid is taken of the plunger and therefore the displacement nut is exposed.

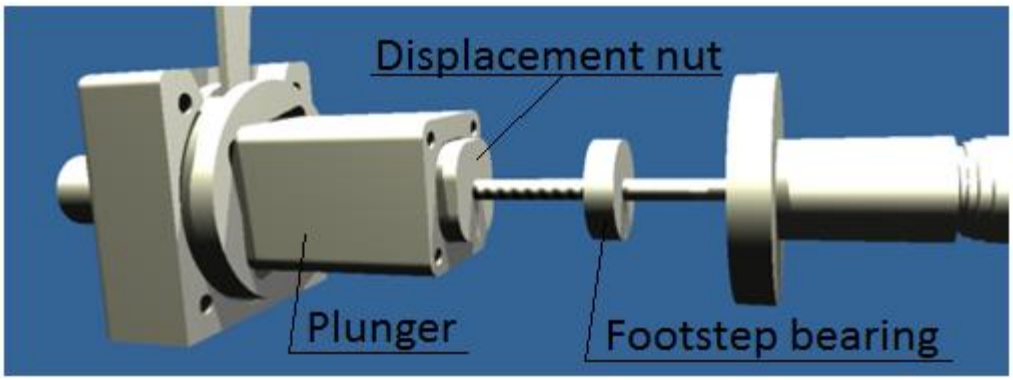

Figure 27: Second shooting system, view on the plunger and spindle

In the first design, it wasn't considered that a large axial force is generated in the spindle. All this force had to be endured by the bearings in the motor. When a large force is applied, this isn't ideal for the endurance of the motor. In this second construction, the axial force is handled by a footstep bearing which presses against the outer body. This is seen in figure 27 and in figure 28, at the end of the guidance bush.

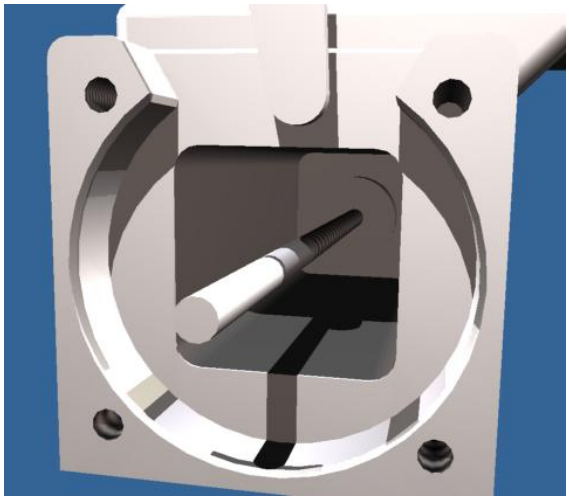

Figure 28: Second shooting system, close-up on the guidance bush and footstep bearing

The actuation of the release ring needs a sufficient amount of torque. The stepper motor used in the first design cannot deliver this amount. In this design, a servomotor is used to increase the amount of torque and to achieve a more accurate positioning of the release ring. This is seen in figure 29.

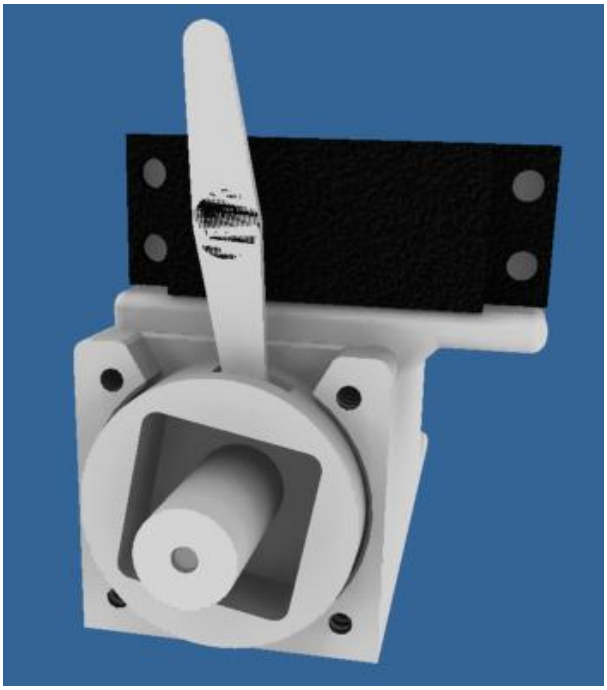

Figure 29: Second shooting system, view on the release ring and servomotor

3.7 Experiments

In order to test the mathematical model, some experiments are performed. In this paragraph, these experiments are discussed.
Before starting the experiments, some comments have to be made. Due to adaptations in the design of the shooting systems, the values from paragraph 3.4.2 can't be used to compare the experiments. Table 5 gives the adapted values from the mathematical model, used to compare to the measured values in the experiments.

Table 5: Adapted values from mathematical model

Description	**Value**
Spring free length	30 mm
Spring compressed length	10 mm
Spring precompressed length	15 mm
Spring stiffness	1500 N/m
Plunger stroke	15 mm
Compressed spring force	45 N
Winding time 0 to 45 N	5,70 sec
Winding time 0 to 22,5 N (precompression)	2,76 sec
Winding time 22,5 N to 45 N	2,93 sec
Ball velocity (5 mm plunger offset)	2,86 m/s
Ball velocity (0 mm plunger offset)	3,14 m/s

3.7.1 Compression process

In a first experiment, the maximum force that the motor can deliver can be measured. This is done by taking a spring with high stiffness, like the selected spring in paragraph 3.4.2.1. From the experiment, it seems that the motor can't deliver this force. An explanation for this fact is that there is friction between the displacement nut and the guidance bush. For the further experiments, a spring with lower stiffness is mounted, so that the motor is able to wind the spring up.
Another important parameter in the compression process is the time to wind the spring up. This time can be measured by starting at zero compression. When the spring is wound up, the motor goes into stall. Therefore, time to achieve the maximum force in the spring is known.
In the model, it is assumed that the force in the spring starts from zero. In the actual shooting system, the spring is precompressed to save space. To compare the measured time with the theoretical time, the time to wind the spring to the precompression force has to be subtracted from the theoretical time.

Table 6: Winding time measurements

Measurement	**Time (s)**
1	4,51
2	4,56
3	4,49
4	4,46
5	4,49
Mean	**4,50**

The compression time, calculated in the model is 2,93 sec. Compared to the measured time of 4,50 sec, this is 35% lower.
In the model, only the friction between spindle and nut is considered. In the real design, the axial forces that work on the spindle causes extra friction. This is the reason why the maximum force can't be reached and that it takes extra time to wind the spring up.
A second reason why the maximum force can't be reached is the non perfect alignment of the motor relative to the spindle. This causes an extra loss in motor torque that can be transferred to the spindle.

3.7.2 Releasing process

3.7.2.1 Release-ring

When the force in the spring reaches the maximum force, the mechanism should be able to release the plunger. Due to high friction forces in the release-ring, this can cause problems. When the friction is too high, the servomotor will not be able to actuate the release-ring.
With the spring, selected in paragraph 3.4.2.1, the friction in the release-ring is too high when the spring is entirely wound up. The servomotor isn't able to turn the ring. For the following tests, a spring with lower stiffness is mounted.
With the lighter spring, the friction in the release-ring is acceptable. The servomotor will be able to turn the ring.

3.7.2.2 Ball velocity

Due to the problems, described in previous paragraphs, a lighter spring had to be mounted. This implicates that the velocity of the ball will be lower than 7 m/s determined in paragraph 3.4.2.1.

Table 7: Ball velocity measurements

Plunger offset (mm)	**Time (s)**	**Distance (m)**	**Velocity (m/s)**
0	1,01	2	1,98
0	0,97	2	2,06
0	0,90	2	2,22
0	0,93	2	2,15
Mean value	**0,95**		**2,10**
5	0,95	2	2,10
5	1,05	2	1,90
5	1,12	2	1,78
5	1,07	2	1,86
Mean value	**1,04**	**2**	**1,92**

In table 7, the time that the ball needs to cover a distance of 2 meters is given. From table 7 it is seen that the mean velocity of the ball with a plunger offset of 5 mm is 1,92 m/s. The maximum velocity calculated in the model is 2,86 m/s (see table 5). The measured mean velocity of the ball with no plunger offset is 2,10 m/s compared to the maximum theoretical velocity of 3,14 m/s (see table 5).
In this experiment, the time it takes the ball to cover a distance of two meters is measured. The accuracy of the measured time is not high because the timer can't be started exactly at the time the ball is shot away.

The velocity that is derived from the measured time is a mean time to cover the distance. In the model, the maximum velocity of the ball is determined which is slightly higher.
Other teams reach a ball velocity of 10 m/s. A velocity of 3 m/s is fit for soccer playing but in order to keep up with the other teams, a higher velocity is required.

3.8 Conclusions

In this chapter, the shooting device is discussed. A comparison between all competing teams was made. In this comparison, it is seen that all teams use a solenoid powered shooting device. For this application, it was decided to develop a mechanical system powered by a spring. Because of the direct coupling between the motor and the shooting system, it is expected that higher efficiency can be achieved but this hasn't been proven yet.
In order to select a spring for the application, a mathematical model is developed. From this model, it can be concluded that the plunger's mass should be kept as low as possible. The offset between the ball and plunger at the start of the shooting process should also be kept as low as possible. Some experiments were performed to compare the model with the reality. It can be concluded that due to friction and non perfect alignment of the motor with the spindle, the model gives an overestimation of the maximum achievable force in the spring. Also due to friction, the model gives an overestimation of the ball velocity.

4 Dribbler

4.1 General

The dribbler is a very important component on the robot. With a good dribbling system, the ball can be handled better. By bringing the ball to the center of the robot, the ball is located right in front of the kicking system. The ball can be kicked more accurate. Some competing teams can make a difference in game-play by a good dribbling system alone.

4.2 State of the art

Table 8: Comparison between RoboCup teams: Dribbler

Team	Dribbler type	Transmission	Motor
Botania Dragon Knights [1]	Cylinder	Spur gear	
Brocks [2]	Cylinder	Spur gear	6 W brushed DC
B-Smart [3]	Cylinder	Belt	Faulhaber 2224U006SR DC Motor
CMDragons [4]	**Cylinder**	**Spur gear**	
Eagle Knights [5]	-Profile -Cylinder	Spur gear	Faulhaber 2224P0212
ER-Force [6]	Cylinder		Maxon A-max 19
Field Rangers [7]	Cylinder	Spur gear	Faul- haber Brushless DC Motor
Immortals [8]	Cylinder	Spur gear	Maxon EC-Max-22 25 W
Khainui [9]	Cylinder	Spur gear	
KIKS [10]	Cylinder	Spur gear	Re-max 24 10 W
KN2C [11]			

ODENS [12]	**Cylinder**		
OMID [13]	Cylinder	Spur gear	Maxon EC16 15 W
Owaribito [14]	Cylinder	Chain	
Parsian [15]	Cylinder	Spur gear	Maxon A-Max22 DC motors 6W
RFC Cambridge [16]			
Robojackets [17]	Cylinder	Spur gear	Maxon EC16 brushless motor
Robodragons [18]	**Cylinder**	**Spur gear**	Maxon EC16 brushless motor 15 W
RoboFEI [19]	Cylinder + profile	Spur gear	Maxon EC22 20W
RoboFighties [20]			
RoboPET [21]	Cylinder		Maxon EC16 BL 15W
Skuba [22]	**Cylinder**	**Spur gear**	
MRL [23]	Cylinder	Spur gear	MAXON EC 16
UBC Thunderbots [24]	Cylinder	Spur gear	MAXON EC 16
Plasma-Z [25]	Cylinder	Spur gear	Maxon EC-max 22 25 W

From table 8, it can be concluded that most teams use a cylindrical dribbler. Some teams add a saving in the middle of the cylinder in order to hold the ball at the longitudinal axis of the robot. One team has used a dribbler-bar with a profiled shape that guides the ball towards the center of the bar.
The gross of used motors have a power rating of 15 to 25 Watts.

4.3 Dimensions of the dribbler

A major concern in designing the dribbler is the '20%' rule which states that the ball can only be covered 20% by the robot. This has a direct effect on the position of the dribbler-bar.

The position of the dribbler can be calculated:

'p' represents the chosen ball coverage with a maximum of 0,2.

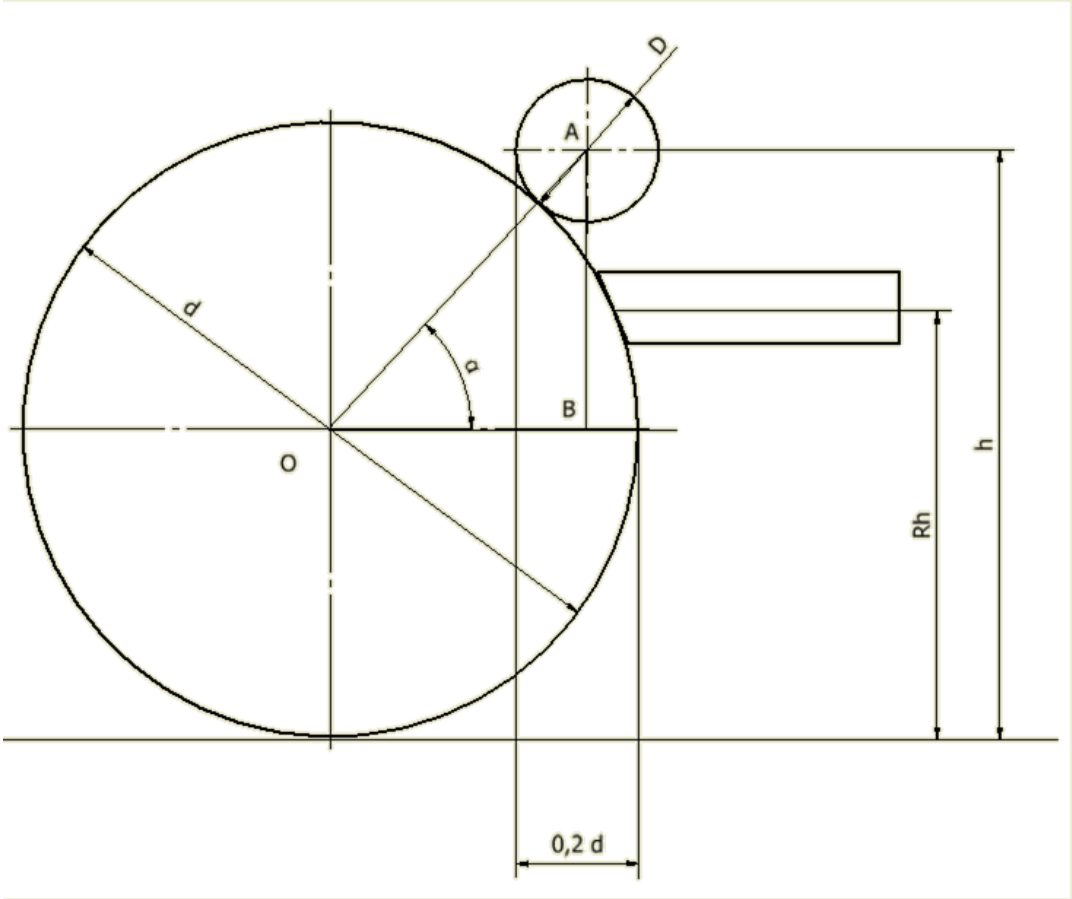

Figure 30: Dribbler setup

The parameters used for deriving a formula are seen in figure 30:

- d : Diameter of the ball = 43 mm
- D : Diameter of the dribbler bar
- R_h: Height of the shooting plunger
- h: Height of the dribbler bar

$$cos\alpha = \frac{OB}{OA} = \frac{\frac{d}{2} - p.d + \frac{D}{2}}{\frac{d+D}{2}} = \frac{d - 2.p.d + D}{d+D} = 1 - \frac{2.p.d}{d+D} \quad (5.1)$$

$$sin\alpha = \frac{AB}{OA} \quad (5.2)$$

The height becomes:

$$h = OA.sin\alpha + \frac{d}{2} \quad (5.3)$$

$$= OA.\sqrt{1 - cos^2\alpha} + \frac{d}{2} \quad (5.4)$$

$$= OA.\sqrt{1 - \left(1 - \frac{2.p.d}{d+D}\right)^2} + \frac{d}{2} \quad (5.5)$$

$$= OA.\sqrt{1 - \left(1 - \frac{4.p.d}{d+D} + \frac{4.p^2.d^2}{(d+D)^2}\right)} + \frac{d}{2} \quad (5.6)$$

$$= \frac{d+D}{2}.\sqrt{\frac{4.p.d}{d+D} - \frac{4.p^2.d^2}{(d+D)^2}} + \frac{d}{2} \quad (5.7)$$

$$\sqrt{\frac{(d+D)^2}{4}.\left(\frac{4.p.d}{d+D} - \frac{4.p^2.d^2}{(d+D)^2}\right)} + \frac{d}{2} \quad (5.8)$$

$$= \sqrt{(d+D).p.d - p^2.d^2} + \frac{d}{2} \quad (5.9)$$

$$= \sqrt{p.d^2 + p.d.D - p^2.d^2} + \frac{d}{2} \quad (5.10)$$

$$= \sqrt{d^2.(p - p^2) + p.d.D} + \frac{d}{2} \quad (5.11)$$

With ball diameter: 43 mm, dribbler-bar diameter: 10mm and p: 20% the height of the dribbler, h, should be 41 mm measured from the ground surface.

4.4 Design

Before starting the design, some comments have to be made:

The most straightforward design is a fixed roller bar connected to the motor with a power transitioning component. When the ball hits a fixed roller bar, it is uncertain that it will stay under the bar.

By making use of a suspended roller bar, the chance that the ball will stay under the bar increases. Because of the limited space in the front of the robot, such a system is difficult to build.

In a first stage, a fixed roller bar is designed for testing purpose. When this system proves insufficient, a suspended system can be designed.

In this application, a belt and pulley transmission system is chosen to power the roller bar. In this case, skid can occur which can capture the impact from the ball instead of transmitting the impact directly to the motor.

In figure 31, all components of the dribbler system are represented in a red color.

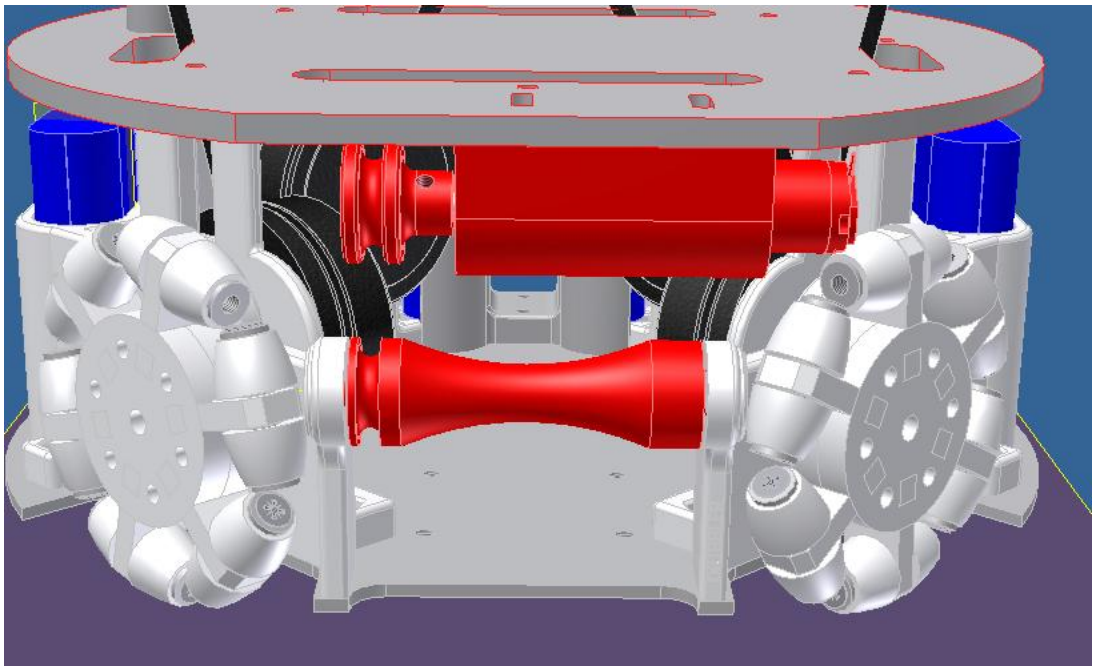

Figure 31: Dribbler components

4.5 Experiments

To evaluate the dribbler system, a simple test can be executed. The robot has to be able to hold the ball in front of it. This is performed in static conditions, so the robot doesn't move during this test.

The current configuration cannot hold the ball in place. When the ball makes contact with the dribbler-bar, it gets pushed away from the bar. A possible solution to overcome this problem is to suspend the dribbler-bar.

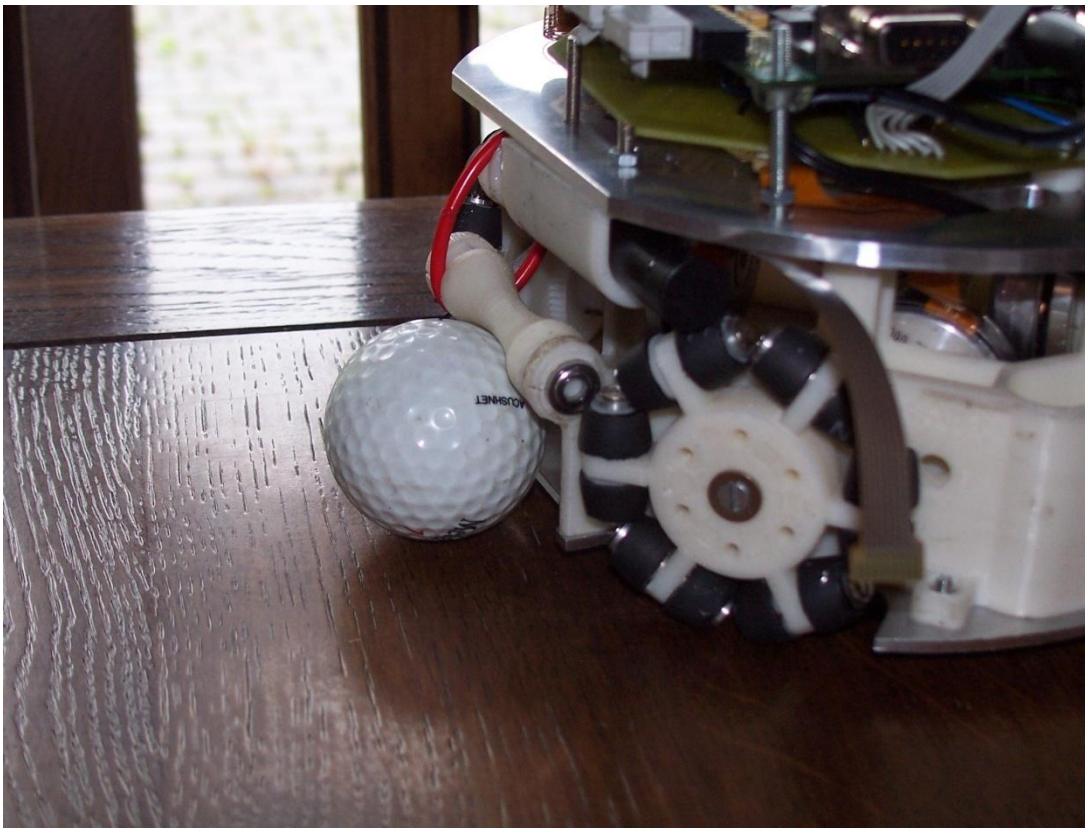

Figure 32: Dribbler experiment

4.6 Conclusions

In this chapter, the dribbler device was discussed. When a comparison between all teams is made, it is seen that they all use a cylindrical dribbler bar. Some teams make a saving in the center of this bar to keep the ball in the center of the robot. In this application, a profile is given to the dribbler bar in order to guide the ball to the center of the robot.

A calculation is made to determine position of the dribbler relative to the ground regarding the 20% rule. This rule states that no more than 20% of the ball can be covered by the robot (thus the dribbler bar). From tests, it is concluded that the dribbler should be suspended in order to control the ball better.

5 Electronics

5.1 Motor controller

5.1.1 Brushless DC drive motors controller

The control of a brushless motor is based on the principle of electronic commutation [30]. Rotor position is reported by three in-built Hall sensors. The Hall sensors are arranged with an offset of 120°. They provide six different signal combinations per revolution. The three partial windings are now supplied in six different conducting phases in accordance with the sensor information. The current and voltage curves are block-shaped. The switching position of each electronic commutation is offset by 30° from the respective torque maximum. Figure 33 gives an overview of the block commutation principle.

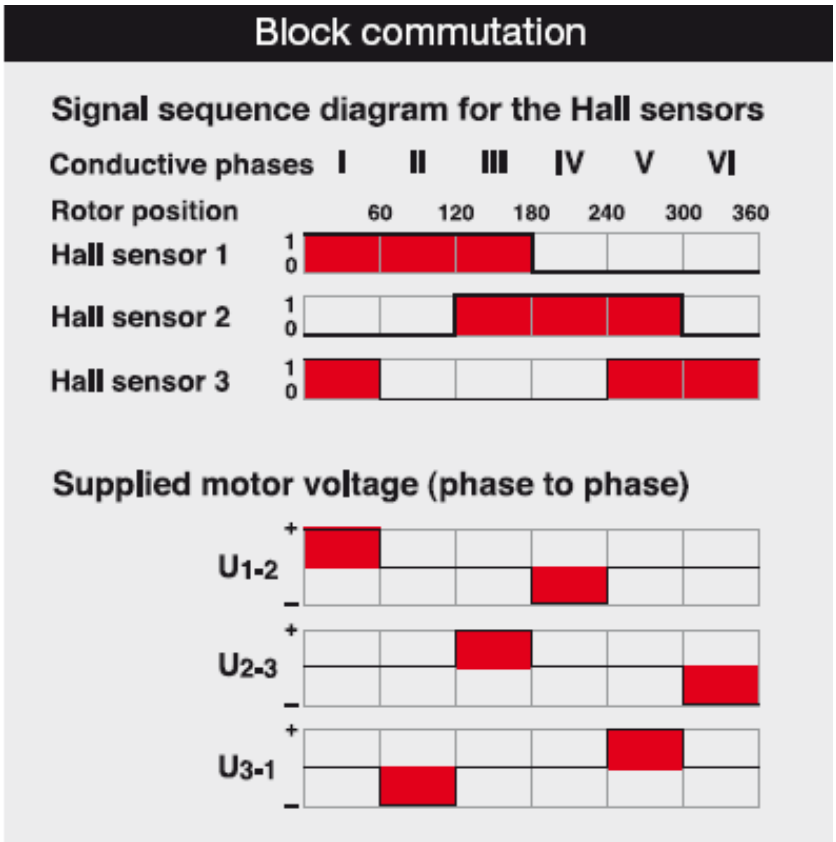

Figure 33: Block commutation for brushless DC motor [30]

A first possible manner of implementing this principle in an electronic circuit is using six transistors which are controlled by the processing unit. In order to do so, a lot of code has to be written. The processor will need some time to process the needed output, especially because four driving motors are used in this application.
In order to reduce the processing time, an electronic component which controls the block commutation can be used. In this application, a L6235 component is used. Compared to other components that were available at our supplier, this component could direct the most current. To use this component, an electronic circuit had to be created.

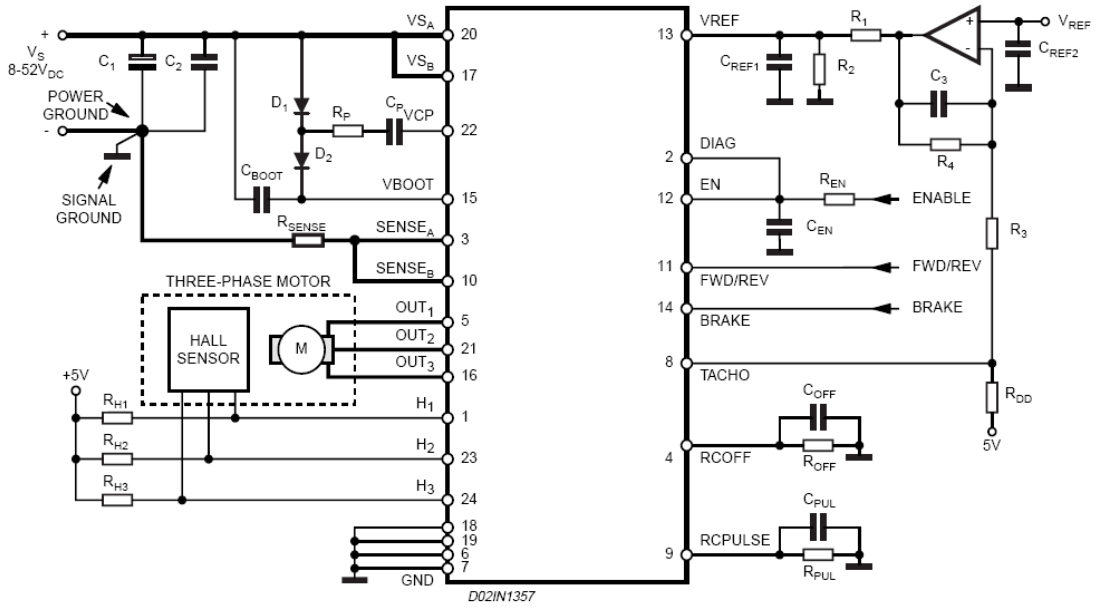

Figure 34: Electronic circuit for brushless motor [30]

The L6235 can be controlled with following signals:

- ENABLE: Enables the current to flow through the motor.
- FWD/REV: Determines the rotation direction of the motor.
- BRAKE: When set low, the rotation of the motor is disabled.
- Vref: Analogue signal which determines the motor speed.
- TACHO The frequency of this signal gives the motor speed.

The circuit shown in figure 34 includes a PID speed control loop connected to the Vref and Tacho pins of the motor driver. This speed control can be made in the software of the FPGA to reduce the size of the circuit. The variables of the PID control can then be set in the software.

5.1.2 Brushed motor for kicking device and dribbler

In order to drive the dribbler and power the kicking system, two brushed DC motors are used. The motor for the dribbler system needs to vary in motor speed. Therefore, a H-bridge is used. The motor for the kicking device doesn't need a variable speed but a reverse rotation direction is needed. The H-bridge can also be used to do so. Figure 35 shows the electronic circuit that has to be built to power the H-bridge. The bridge used is a L6203 full H-bridge.

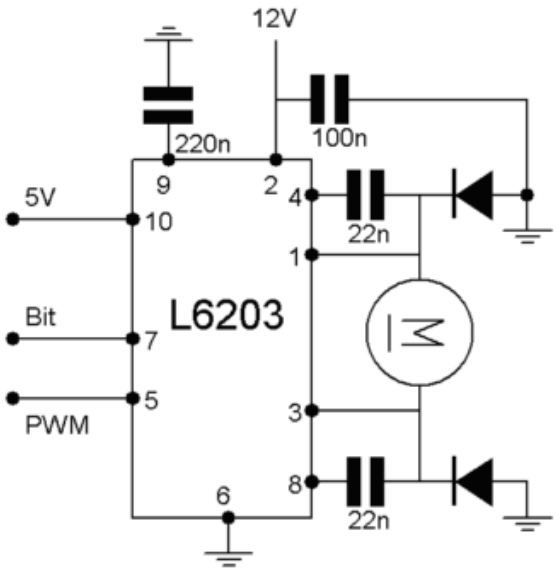

Figure 35: H-bridge for brushed motor

5.2 Interface electronics

5.2.1 FPGA

The FPGA used is a Spartan 3 starter board from Digilentic. All details can be found in the datasheets [34]. Our interests goes to the input and output possibilities, the clock which is used , the memory, the possibility to save a program in its memory and the instructions needed to program the controller. Some specifications of the FPGA used are:

- Internal clock frequency: 500 MHz
- Flash program memory: 2 Mb
- Data memory: 216 Kb
- Input/output pins: 3x40-pin expansion ports
- Display: 4-digit, 7-segment
- Extra input: 8 slide-switches, 4 pushbuttons
- Extra output: 9 LED’s

The uploaded program doesn’t remain in the FPGA’s memory when the power is cut off. For testing purposes, this doesn’t cause a problem yet. In a later stage of this project, a solution has to be found to keep the program in memory.

5.2.2 Voltage regulation

The +12V supplied by the battery is converted into a stable +5V using a 7805CT voltage regulator. The +5V is needed to supply the FPGA. Other components that use the +5V are the Hall sensors in the brushless drive motors.

5.3 Experiments

A first experiment was performed where the motor was powered at full power with no load. This didn't cause any troubles. When the motor speed was reduced by applying a PWM-signal (pulse width modulation) the motor drivers started to heat up. It didn't take long before they were destroyed. After many tries, it was decided to remove the over current protection i.e. the capacitor on the enable pin.
The overcurrent protection is to sensitive. This causes the motor controller to switch off several time per second. Therefore, extra switching of the IGBT's inside is required with extra heating as a consequence.

5.4 Conclusions

In this chapter, the electronics for the robot are discussed. A circuit to control the brushless drive motors was built using a L6235 motor controller. Many problems occurred when implementing this motor controller. When a PWM signal was put on the V_ref pin, the controller started to heat up. This problem was overcome by removing the overcurrent protection.
Another circuit was built to control the dribbler and shooting device motors. Therefore, a L6203 full H-bridge was used.
A FPGA is used for the low level control of the robot. This FPGA provides all required signals for the brushless motor controller, dribbler controller and shooting device controller. A major disadvantage of this FPGA is that the implemented software does not remain in memory when the power is shut off.

6 Software

6.1 Motion control

6.1.1 General

The high level control provides the robot with the needed signals trough a wireless network. The signals that are sent to the robot depend on the type of high level control. Some teams are reducing the processing time on the robot by implementing the robot control in a complete high level control. The velocity signal for each motor is send through the network. This type of control reduces the needed processing capacity on the robot but gives extra load to the off-field PC and wireless communication system.

Another type of high level control provides the robot with the desired motor speeds. The processing unit on the robot will determine a velocity signal regarding the actual velocity and the desired one. This is an intermediate solution because the processing tasks are divided between the off-field PC and the robot's processing unit.

In a last type of control, the off-field PC will only send the desired relative position, the desired rotation-angle and the available time to take these actions. The processing unit on the robot will convert the signals into a velocity signal for each motor. Therefore, this is a complete low level control. For this type of control, the processing unit on the robot will need a lot of calculating time.

For this application, the last type of control is selected in order to have compatibility with the work done by other thesis students.

6.1.2 Electronic compass

The selected type of high level control requires the knowledge of the rotation angle of the robot. This can be measured using the overhead camera but that will result in extra processing time of the off-field PC. Another manner of measuring the angle is by using an electronic compass like the Hitachi HM55B compass [33].

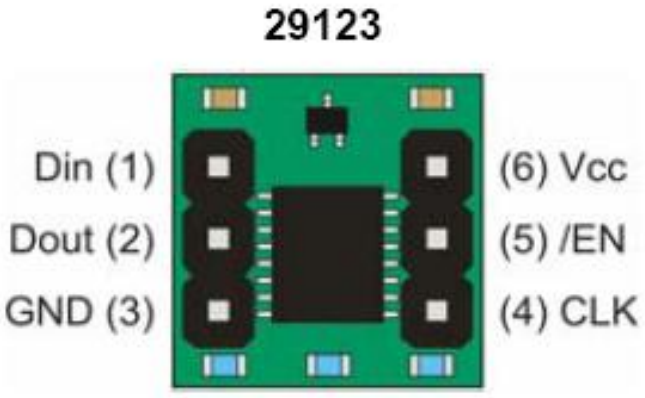

Figure 36: Hitachi HM55B connection scheme

The CLK-pin of the compass has to be connected to a clock signal of the FPGA. The EN-pin is an active-low device enable.
In order to measure the angle, some commands have to be send to the Din pin of the compass:

Table 9: Electronic compass commands

Binary value	Action
0000	Reset device
0001	Start measurement
0011	Report measurement

6.1.3 Motor speed estimation

A speed estimation of the motor can be achieved by using one of the Hall-sensor outputs. With the help of the L6235 motor driver, the speed estimation is made easier. The period of the 'tacho' output can be measured by using the FPGA. A counter starts to run when a rising edge of the Hall-sensor output is registered and resets when a second rising edge is detected. Knowing the FPGA's clock is working at 50MHz, the speed is determined.

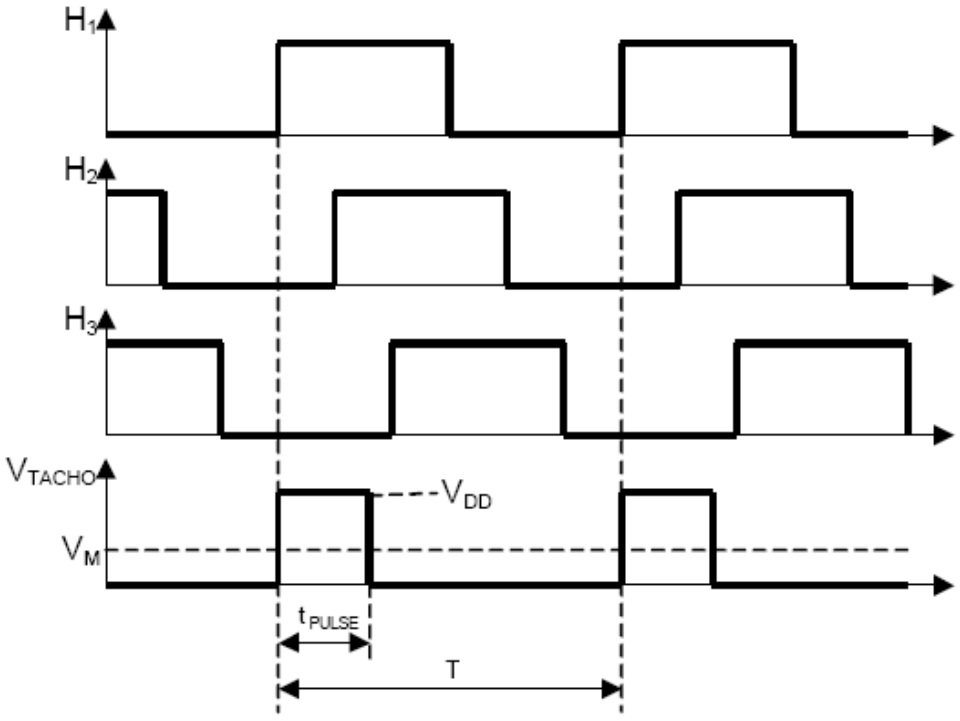

Figure 37: Speed estimation using the L6235 motor driver

6.1.4 Motor control

A successful team that uses a complete high level control is the Skuba-team [22]. In a complete low level control, the rotation angle has to be measured with the electronic compass. The velocity commands have to be retrieved from the relative displacement and the available time to take the actions. When these are determined, the rest of the calculation remains equal to the complete high level control. In this paragraph, the control performed by the Skuba-team is explained. Normally, when the off-field PC sends the velocity command to the robot, it doesn't perform any velocity feedback control and it assumes that the robot's motion controller has already taken care of this. Due to the loss from friction, wheel slippage and other real world problems, the robot cannot move as fast as commanded.

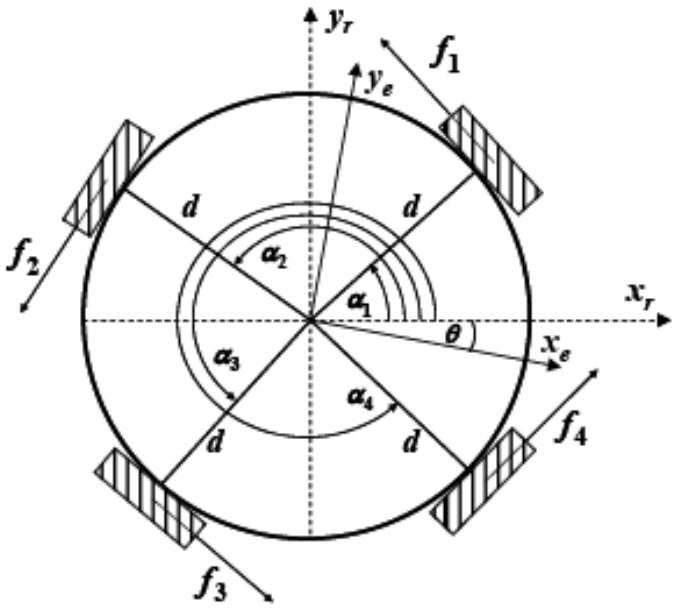

Figure 38: Robot layout for motor control

The normal kinematics can be written as:

$$\zeta_{\mathrm{r}} = \psi . \zeta_{\mathrm{desired}} \tag{6.1}$$

Where,

$\zeta_r = [\dot{\varphi}_1 \quad \dot{\varphi}_2 \quad \dot{\varphi}_3 \quad \dot{\varphi}_4]$ the representation of the linear velocity of the wheels.

$\zeta_{desired} = [\dot{x} \quad \dot{y} \quad \dot{\theta}]$

$$\psi = \begin{bmatrix} \cos\theta . \sin\alpha_1 + \cos\alpha_1 . \sin\theta & \sin\theta . \sin\alpha_1 - \cos\alpha_1 . \cos\theta & -\mathrm{d} \\ \cos\theta . \sin\alpha_2 + \cos\alpha_2 . \sin\theta & \sin\theta . \sin\alpha_2 - \cos\alpha_2 . \cos\theta & -\mathrm{d} \\ \cos\theta . \sin\alpha_3 + \cos\alpha_3 . \sin\theta & \sin\theta . \sin\alpha_3 - \cos\alpha_3 . \cos\theta & -\mathrm{d} \\ \cos\theta . \sin\alpha_4 + \cos\alpha_4 . \sin\theta & \sin\theta . \sin\alpha_4 - \cos\alpha_4 . \cos\theta & -\mathrm{d} \end{bmatrix}$$

Desired robot velocity ($\zeta_{desired}$) is used to generate robot's wheel angular velocity vector (ζ_r). This wheels angular vector is the control signal which is sent from PC to interested mobile robot.

The regular robot kinematics describes an ideal situation where there's no system disturbance. In order to control the robot more accurately, the robot kinematics is modified with disturbance parameters. The friction force and traction torque vector are defined. The output linear velocity ($\zeta_{observed}$) is observed by a bird eye view camera. The output velocity contains information about disturbances, therefore by comparing the desired velocity and the output velocity. The output velocity can be defined as (6.2) when assuming that disturbance is constant for the specific surface. The two disturbances are modeled.

$$\zeta_{\mathrm{observed}} = (\psi^{\dagger} + \epsilon) . \zeta_{\mathrm{r}} + \Delta \tag{6.2}$$

Where,

$\psi^{\dagger}$ Is the pseudo inverse of the kinematic equation.

ε is the disturbance gain matrix due to the robot coupling velocity friction.

Δ is the disturbance vector due to the surface friction.

The disturbance matrices can be found from experiments. The experiments performed by the Skuba-team [22] are used as an example. From the data they

measured last year, the disturbance vector of the surface friction is constant but the coupling velocity friction is a nonlinear function with respect to the robot translation and angular velocity. With these two disturbance parameters, the robot command can be compensated and result in the actual robot output velocity command. The surface friction can be found by using two observed experimental data while the coupling velocity friction matrix can be estimated using the calibration software. The software performs the experiment by running the robot at different speeds and observing the output velocity from the robot. Then, the disturbance ε can be estimated by using a second order polynomial least squares fitting method. By using modified kinematics to generate the control command, the robot can move more accurately. The comparison of the experimental result is shown in figure 39. The graphic at the top represents the normal kinematics, the bottom graphic represents the modified kinematics.

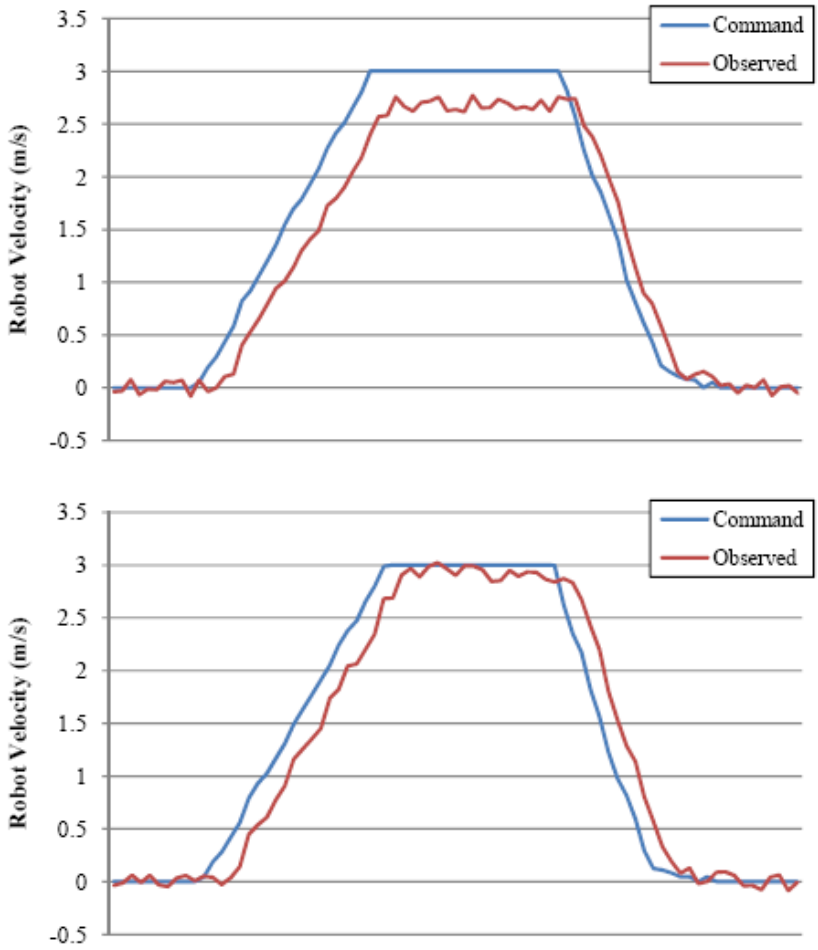

Figure 39: Experimental results for modified kinematics performed by Skuba-team [22]

6.2 Kicking device control

As seen in paragraph 4.3, the force generated in the spring is function of the motor speed. The speed control of this motor doesn't have to be variable because the maximum power of the motor is required at all times. Due to the increase of generated force, the motor speed will decrease.
By measuring the motor speed, a value for the generated force in the spring can be derived. The maximum force is generated when motor speed is zero. When motor speed is equal to the nominal speed, no force is generated in the spring. By assuming that the force will increase linear with decreasing motor speed, the value for the generated force is determined.
When the motor speed is represented by a binary number, each bit is inverted to calculate the generated force.

When the desired force in the spring is achieved, the servomotor of the kicking device is actuated to release the plunger when needed.

To retrieve the plunger, the rotation direction of the motor is inverted. When the plunger is fully retrieved, the motor speed will drop to zero. At this point, the motor should be disabled and the servomotor should be placed in the original position.

6.3 Dribbler control

The speed of the dribbler motor should be variable. When the robot is moving forward, the speed of the dribbler bar should increase to maintain the same backspin of the ball. The dribbler-bar should turn at maximum speed when the robot moves sideways to keep the ball in the center of the robot. Therefore, a variable speed of the dribbler bar should be achieved independent of the driving motor speed of the robot.

6.4 Conclusions

Due to the problems with the motor controller, the motion control wasn't implemented on the robot. Therefore, no experiments could be made to verify this control. Nevertheless, it can be concluded that other teams used this motion control approach with success.

The dribbler control wasn't implemented. It took a long time to get the drive motors working without destroying the motor controllers. Therefore, no experiments could be executed with the dribbler while the robot is moving.

7 Conclusions and further work

7.1 Conclusions

The goal of this thesis is to develop the mechatronic design of a soccer-playing robot for the RoboCup Small Size League. Such a design includes the transmission system, a shooting system and a dribbler. The dimensions of the robot are limited by the rules of play. Implementing all the components in a small amount of space is a real challenge.

After a comparison between the competing teams, the number of wheels on the robot for this application is set to four. A brushless motor of 30 Watt powers the transmission system. The omni-directional wheels mounted on the robot provide a great maneuverability. They come in numerous possible designs. In this application, a combination of these designs is made to come to a new design. There are four wheels mounted on the robot. Thereby, more space is made available for the shooting system. Some variations of the transmission system were designed. From tests, it is concluded that a spur gear transmission is the best option for this application. In order to control the speed of the brushless drive motors, a L6236 motor driver is implemented on the robot. In the first tests, these drivers heated up when a PWM signal was assigned to the v_ref pin. By removing the overcurrent protection, this problem was overcome. A fully variable drive can now be achieved without heating the motor drivers to their breaking point.

Most teams use a solenoid powered shooting system. In this application it was decided to develop a mechanical system with a spring. A mathematical model was developed to simulate the effects of the spring stiffness, the plunger mass and the offset between the ball and plunger. To test this model, a few shooting system designs were developed. From these tests, it can be concluded that the model gives a good guideline for the design but the accuracy can be improved. Due to friction in the shooting system, the values calculated by the model are an overestimation compared to the real ball velocity. Two shooting system designs were developed. The second design can propel the ball with an average speed of 2 m/s.

The dribbler system exists of a dribbler bar with a profile to guide the ball towards the center of the robot. Tests show that with the current design the ball bounces off the bar. A suspension system can avoid this problem.
The basis for the low level control is made but not tested yet. Other teams use the same approach of control with success.

7.2 Further work

The work on this project isn't done yet. It will take some optimization of the robot to achieve the goal of designing a complete robotic system to compete in the RoboCup Small Size League.

On the field of the mechanical design, some improvements can be made. By suspending the wheels, the contact between the wheels and ground surface can be ensured. The dribbler can also be suspended to improve the ball handling. The shooting system must be optimized to reach a ball velocity of 10 m/s.

On the field of the electronic design, some optimization can be done. The size of the motor control PCB can be reduced. Therefore, more space will become available for other components. The interfaces with the outside world can be improved. A connection on the robot's shell to program the FPGA makes the robot user friendly. Also a connection can be made to charge the batteries. The robot has to communicate with an off-field PC by a wireless communication system.

On the field of the software, some more implementations are required. The control loop for the drive motors, shooting system and dribbler have to be implemented. This project is divided into subprojects. The interfaces between the work done by other team members has to be taken care of. An example of such an interface is the development of a communication protocol between the off-field PC and the robots.

8 Appendix

8.1 Appendix A: Rules of play

In this appendix, the rules that are important for the design of the robot are summarized. Most of these rules are directly inherited from regulations provided by the RoboCup organization.

8.1.1 External equipment provided by RoboCup

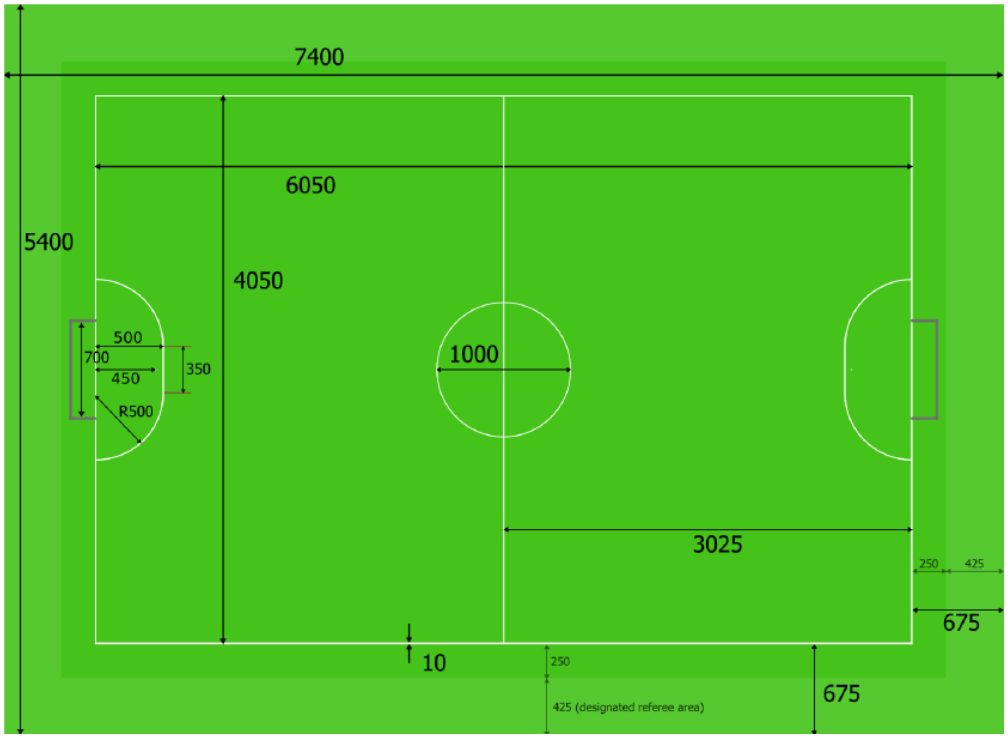

Figure 40: Layout of the playing field

The dimensions of the field are given in figure 40. The playing surface exists of a green felt mat or carpet. The floor under the carpet is flat, level and hard.
The use of a carpet implicates that a contamination of the robot wheels and gears is possible. The design of the robot has to take this into account.
The ball is a standard orange golf ball, has a weight of 46 gram and a diameter of 43 mm.

8.1.2 Robot and internal equipment

8.1.2.1 General

The robotic equipment is to be fully autonomous. Human operators are not permitted to enter any information into the equipment during a match, except at half time or during a time-out.

A robot must not have in its construction anything that is dangerous to itself, another robot or humans.

Robot wheels (or other surfaces that contact the playing surface) must be made of a material that does not harm the playing surface. Metal spikes and Velcro are specifically prohibited for the purpose of locomotion.

8.1.2.2 Dimensions

A robot must fit inside a 180 mm diameter cylinder and have a height of 150 mm or less. Additionally, a robot's top area must adhere to the Standard Pattern size and surface constraints as described in the rules of play.

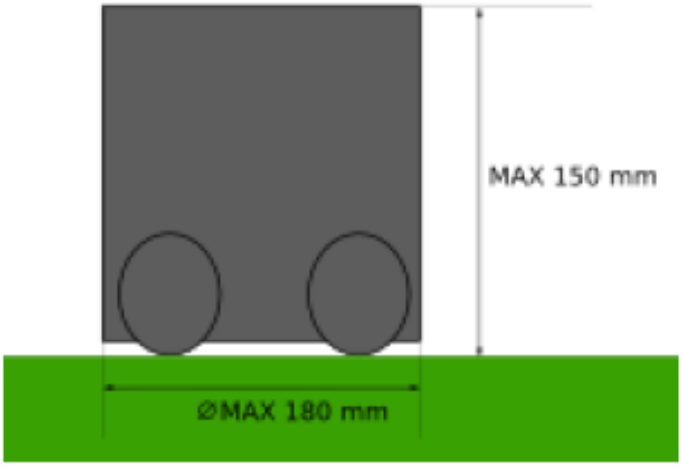

Figure 41: Maximum dimensions of the robot

8.1.2.3 Recognition pattern

Before a game, each of the two teams has a color assigned, namely yellow or blue. All teams must be able to be either yellow or blue color. The assigned team color is used as the center marker color for all of the team's robots. The detailed layout of the markers is described in the section "Standard Pattern" of the rules of play.
All participating teams must adhere to the given operating requirements of the shared vision system. In particular, teams are required to use a certain set of standardized colors and patterns on top of their robots. To ensure compatibility with the standardized patterns for the shared vision system, all teams must ensure that all robots have a flat surface with sufficient space available on the top side. The color of the robot top must be black or dark grey and have a matte (non-shiny) finish to reduce glare. The SSL-Vision standard pattern is guaranteed to fit within a circle of radius 85mm that is linearly cut off on the front side of the robot to a distance of 55mm from the center. Teams must ensure that their robot tops fully enclose this area.

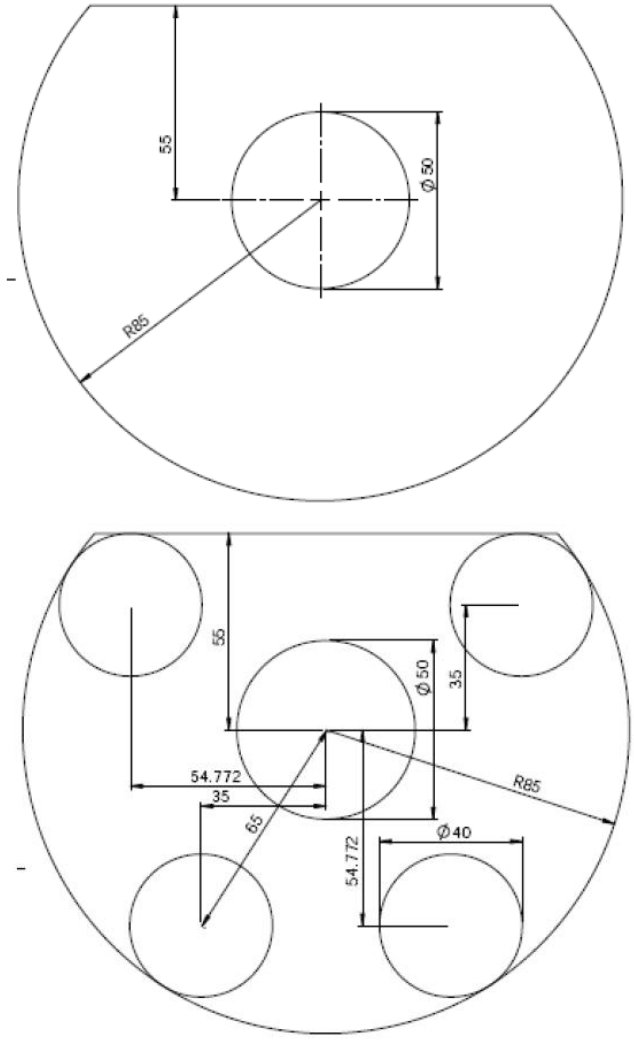

Figure 42: Dimensions of the recognition pattern

Teams must make sure to still adhere to the standard robot top area size. Each robot must use the standardized pattern with a unique color assignment selected from a standardized set of possible color combinations. No two robots are allowed to use the same color assignment. The center dot color determines the team and is either blue or yellow. Standardized colored paper or cardstock for all required colors will be provided at the competition. The set of legal color assignments is shown in figure 43.

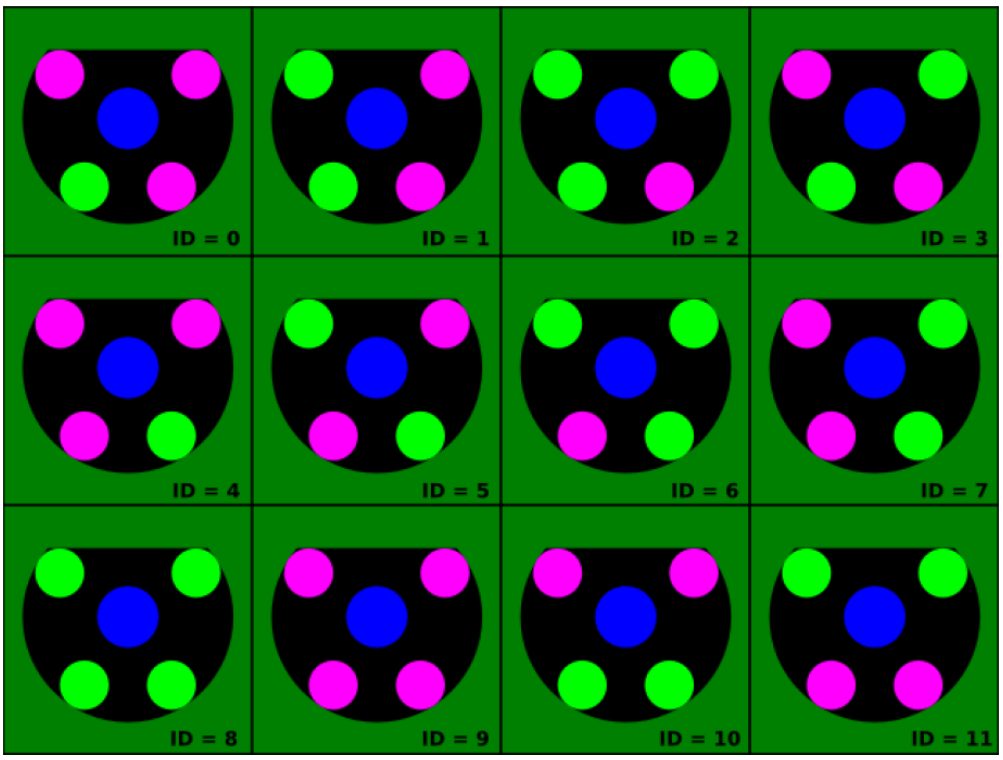

Figure 43: Legal color assignments

Teams are encouraged to select color assignments with ID 0-7 because they have been experimentally found more stable, as there is no risk that the back two dots "color-bleed" into each other.

Official colors will be provided by the organizing committee. Teams must use the official colors unless both teams agree not to.

8.1.2.4 Dribbler

Dribbling devices that actively exert backspin on the ball, which keep the ball in contact with the robot are permitted under certain conditions. The spin exerted on the ball must be perpendicular to the plane of the field. Vertical or partially vertical dribbling bars, also known as side dribblers, are not permitted.

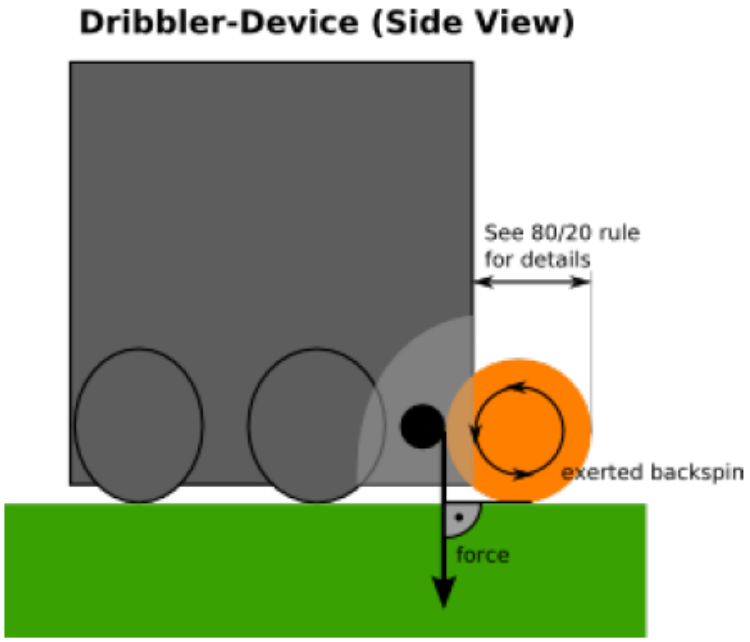

Figure 44: 20% rule

Adhesives such as glue or tape may not be used for the purpose of ball control or to construct dribblers. Dribbling devices which use such an adhesive to affix the ball to a robot are considered a violation of Law 12, Decision 4, by "removing all of the degrees of freedom of the ball". In addition, the use of adhesives for any purpose on the robot which results in residue left on the ball or field, is considered as damage and sanctioned as per Law 12.
An indirect free kick is awarded to the opposing team if a robot dribbles the ball over a distance greater than 500 mm

8.1.2.5 Kicking device

Kicking devices are permitted.

The current rule about scoring after chip kicks is defined in this section (subsection Indirect Free Kicks) only. During past competitions, some confusions occurred after robots chipped the ball and thereby caused own goals. For this reason, a strict interpretation of this rule is provided here:

If a robot chips the ball (no matter at which height it travels) at a team mate and the ball subsequently enters the own goal, the opponent team scores.

If a robot chips the ball at an opponent and the ball subsequently enters the own goal while staying below 150mm all the time after touching the opponent robot, the opponent team also scores.

If a robot chips the ball at an opponent and the ball subsequently enters the own goal after having been above 150mm for some time (and not being in constant touch with the ground afterwards) after touching the opponent robot, the opponent team does not score.

An indirect free kick is also awarded to the opposing team if a robot touched the ball such that the top of the ball travels more than 150 mm from the ground, and the ball subsequently enters their opponent's goal, without having either touched a teammate (while below 150 mm) or remained in contact with the ground (stopped bouncing).

An indirect free kick is also awarded to the opposing team if a robot kicks the ball such that it exceeds 10 m/s in speed

8.1.2.6 Communication

Robots can use wireless communication to computers or networks located off the field.

Participants using wireless communications shall notify the local organizing committee of the method of wireless communication, power, and frequency. The local organizing committee shall be notified of any change after registration as soon as possible. In order to avoid interference, a team should be able to select from two carrier frequencies before the match. The type of wireless communication shall follow legal regulations of the country where the competition is held. Compliance with local laws is the responsibility of the competing teams, not the RoboCup Federation. The type of wireless communication may also be restricted by the local organizing committee. The local organizing committee will announce any restrictions to the community as early as possible.

Bluetooth wireless communication is not allowed.

8.2 Appendix B: CD rom

Because of the large amount of extra files, they are collected on a CD rom.

Autodesk Inventor Drawings

This map contains all inventor drawings of the robot design. The drawings are arranged by component.

Electronic circuit

This map contains the electronic circuits developed with Traxmaker.

Matlab

This map contains the Matlab files:

- Shooting system
    - Calculation of maximum force
    - Compression process
    - Releasing process

9 Bibliography

9.1 Team description papers

1. **Liu, Yang.** Botnia Dragon Knights. *Team Description Paper for RoboCup 2010 Small Size League.* Vaasa, Finland : Vaasa University of Applied Sciences, 2010.

2. **M. Akar, ¨ O. F. Varol, F. ˙Ileri, H. Esen, R. S. Kuzu and A. Yurdakurban.** BRocks 2010 Team Description. Istanbul, Turkey : Bogazici University, 2010.

3. **Tim Laue, Sebastian Fritsch, Kamil Huhn, Arne Humann, Michael Mester, Jonas Peter, Bastian Reich, Max Trocha.** B-Smart. *Team Description for RoboCup 2010.* Bremen, Germany : Deutsches Forschungszentrum fur Kunstliche Intelligenz GmbH, 2010.

4. **Stefan Zickler, Joydeep Biswas, Kevin Luo, and Manuela Veloso.** CMDragons 2010 Team Description. Pittsburgh,USA : Carnegie Mellon University, 2010.

5. **Ernesto Torres, Paolo Aguilar, Alan C´ordova, Hip´olito Ruiz, Julio S´anchez, Miriam Mart´ınez, Marco Morales, Matthew Holland, Wayne Blackshear, Chris Hewell, and Alfredo Weitzenfeld.** Eagle Knights. *Robobulls 2010: Small Size League.* Mexico City, Mexico : Robotics Laboratory, Division of Engineering ITAM, 2010.

6. **Peter Blank, Michael Bleier, Jan Kallwies, Patrick Kugler, Dominik Lahmann, Philipp Nordhus, Christian Riess.** ER-Force. *Team Description Paper for RoboCup 2010.* Erlangen, Germany : University of Erlangen-Nuremberg, 2010.

7. **Yusuf Pranggonoh, Buck Sin Ng, Tianwu Yang, Ai Ling Kwong, Pik Kong Yue, Changjiu Zhou.** Field Rangers. *Team Description Paper.* Singapore : Advanced Robotics and Intelligent Control Centre (ARICC), 2010.

8. **Mohammad Reza Niknejad, Seyed Ali Salehi Neyshabouri, Seyed Ali Ghazi MirSaeed, Ehsan Kamali, Mohammad Hossein Fazeli.** Immortals. *2010 Team Description Paper.* Iran : Iran University of Science and Technology, 2010.

9. **Srikluan M., Srithong A., Prisuwun S., Paocharoen J., Chaiburee W., and Karnjanadecha M.** Khainui Team Description for Robocup 2010. Songkhla, Thailand : Prince of Songkla University, 2010.

10. **Ryuhei Sato, Takato Horii, Kenji Inukai, Shoma Mizutani,Kosei Baba, Masato Watanabe, Kazuaki Ito and Toko Sugiura.** KIKS 2010 Team Description. Japan : Toyota National College of Technology, 2010.

11. **Milad AbaeiRad, Majid Ahady, Sayyed Ata-o-llah Khadivi, Salar Moghimi, Faraz Fallahi, Mostafa SaeediMehr, Adel HeydarAbadi.** KN2C Small Size Team Description Paper. Iran : K.N.Toosi University Of Technology, 2010.

12. **Makoto Nakajima, Takaumi Kimura, Yasuhiro Masutani.** ODENS 2010 Team Description. Osaka, Japan : Osaka Electro-Communication University, 2010.

13. **Mojtaba Najafi, Mahdi Hosseinzadeh, Sajjad Manoochehri, Asadollah Kiaei, Mostafa Abdulghafar,Abbasali Forouzideh, Saeed Alikhani,Ehsan Darestani, Seyed Mahdi Nasiri, Seyed Arman Alaei.** OMID 2010 Team Description Paper. Iran : Shahed University of Tehran,, 2010.

14. **Yasunori NAGASAKA, Morihiko SAEKI, Takuya SOGO, Shoichi SHIBATA, Hironobu FUJIYOSHI, Takashi FUJII, Yoshiyuki TANAKA, Masafumi JYOUO, Takumi ADACHI, Masaki ITO, Kazuhiro SUZUKI, Kazuo TAUCHI, Chikara INUKAI, and Alfred EBADE EFOSA.** Owaribito-CU 2010 Team Description. Japan : Chubu University, 2010.

15. **Valiallah Monajjemi, Seyed Farokh Atashzar, Vahid Mehrabi, Mohammad Mehdi Nabi, Ehsan Omidi, Ali Pahlavani, Seyed Saeed Poorjandaghi, Erfan Sheikhi, Ali Koochakzadeh, Hamid Ghaednia, S. Mehdi Mohaimanian Pour, Arash Behmand, Hamed Rastgar, e.a.** Parsian. *Team Description for Robocup 2010.* Tehran, Iran : Amirkabir Univ. Of Technology, 2010.

16. **Alexei Colin, Svilen Kanev, David Robinson, Rui Jin, Jesse Thornburg, Benjamin Johnson, Aaron Ramirez, Julie Henion, Scott Crouch, Daniel Lynch, Julie Xie, Jesse Yang, Marcel Thomas, Evelyn Park.** RoboCup Team Description Paper. *RFC Cambridge.* Cambridge, USA : Massachusetts Institute of Technology and Harvard University, 2010.

17. **Alex Cunningham, Andrew Bardagjy, Stefan Posey, Ben Johnson, Stuart Donnan, Philip Rogers, and Stoian Borissov.** RoboJackets 2010 Team Description Paper. Atlanta, Georgia, USA : Georgia Institute of Technology, 2010.

18. **Akeru Ishikawa, Takashi Sakai, Jousuke Nagai, Toro Inagaki, Hajime Sawaguchi, Yuji Nunome, Kazuhito Murakami and Tadashi Naruse.** RoboDragons 2010 Team Description. Aichi, JAPAN : Aichi Prefectural University,, 2010.

19. **Jose Angelo Gurzoni Jr., Eduardo Nascimento, Daniel Malheiro, Felipe Zanatto, Gabriel Francischini, Luiz Roberto A. Pereira, Milton Cortez, Bruno Tebet, Samuel Martinez, Reinaldo A. C. Bianchi, and Flavio Tonidandel.** RoboFEI 2010 Team Description Paper. Sao Bernardo do Campo, Brazil : Centro Universitario da FEI, 2010.

20. **Ahmad, Dr. Kanwar Faraz.** Team RoboFighties (Pakistan). Rawalpindi, Pakistan : National University of Sciences and Technology, 2010.

21. **Acauhã dos Santos Fialho, Arthur Crippa Búrigo, Bruno Jurkovski, e.a.** RoboPET Team Description Paper. Porto Alegre, Brazil : Universidade Federal do Rio Grande do Sul (UFRGS), 2010.

22. **Piyamate Wasuntapichaikul, Jirat Srisabye, and Kanjanapan Sukvichai.** Skuba 2010 Team Description. Bangkok, Thailand : Kasetsart University, 2010.

23. **Maziar Ahmad Sharbafi, Mohammad Hoshyari, Saeed Esmaeelpourfard, Omid Bakhshande Babersad, Mohammad Haajseyedjavadi, Danial Esmaeeli.** MRL Team Description 2010. Qazvin, Iran : Islamic Azad University of Qazvin,, 2010.

24. **Alim Jiwa, Byron Knoll, Christopher Head, Howard Hu, Jonathan Fraser, Jonathan rion , Kevin Baillie, Lok Tin Lam.** 2010 Team Description Paper: UBC Thunderbots. Vancouver, Canada : The University of British Columbia, 2010.

25. **Chitchanok Chuengsatiansup1, Thiraphat Charoensripongsa1, e.a.** PlasmaZ. *Extended Team Description Paper.* Bangkok, THAILAND : Chulalongkorn University, 2010.

9.2 Books

26. **Wilhelm Matek, Dieter Muhs, Herbert Wittel, Manfred Becker.** *Roloff/Matek, machine-onderdelen.* Schoonhoven : Academic Service, 1996. 90 395 0482 2.

9.3 Papers

27. **Anam-dong Sungbuk-gu.** Design and construction of continous alternate wheels for an omnidirectional mobile robot. Seoul, Korea: Korea University, 2003.

28. **C.J. Zandsteeg**, Design of a Robocup Shooting Mechanism. The Netherlands: University of Eindhoven

9.4 Websites

29. Small Size Robot League. [Cited: Mei 1, 2010.] http://small-size.informatik.uni-bremen.de/.

9.5 Datasheets

30. Datasheet, “DMOS driver for three-phase brushless DC motor”, www.st.com

31. Datasheet, “DMOS full bridge driver”, www.st.com

32. Datasheet, “Maxon DC motor and Maxon EC motor, key information’, www.maxonmotor.nl

33. Datasheet, “Hitachi HM55B Compass Module”, www.parallax.com

34. Datasheet, “Spartan-3 Starter Kit Board User Guide”, www.digilentic.com